DELFT UNIVERSITY OF TECHNOLOGY

BACHELOR END PROJECT

Transmembrane signal transduction

A comparison between two opposing receptor mechanisms

Tim Vogel

Supervised by:

Dr. J.L.A DUBBELDAM

Dr. T. IDEMA

February 19, 2019

Abstract

In biological cells, information from the external environment of the cell is used to make survival related decisions. For these decisions, it is important that signals are accurately transduced from the outside to the inside of the cell. In *Dictyostelium discoideum*, two opposing mechanisms using G-protein coupled receptors are used for this signalling: the precoupling mechanism, where second messenger molecules bind to the receptor before a ligand binds to it, and the collision coupling mechanism, in which the ligand binding comes first. In this paper, we investigated both models by analyzing how accurately they detect ligand bindings when different receptors are able to interact with each other. A similar analysis is done for returning messenger molecules. We found that the influence of receptors upon each other is low if the receptors operate under the same conditions. However, when the conditions are heterogeneous, the influence of receptors on each other is huge. The main reason for this influence is that ligand binding receptors which are more likely to get detected by messenger molecules will receive more of those messengers, because of their high diffusion rate. The effect of returning messenger molecules on the receptor signal was that ligand detection became possible at times where they otherwise would not be able to be detected anymore, given a replace rate which is low compared to the rate of binding and unbinding of a ligand to a receptor.

Preface

This report is written as part of my thesis project for the combined bachelor of Applied Mathematics and Applied Physics at the Delft University of Technology. Looking back on the time I worked on this project, I look back on a time in which I have learned a lot on a variety of topics (some of these being: receptor mechanisms, mathematical modeling, efficient programming, but there are many more), all while also having fun. In this report, I document my findings while working on this project, together with the methods used to get these findings. I also, where possible, try to find explanations for the properties of the models I find.

During this project, I have had support from many people. First, I would like to thank my supervisors, Johan Dubbeldam and Timon Idema. Johan Dubbeldam, for handing me this project and our weekly meetings, in which we discussed the problems I encountered. Timon Idema, for giving me the opportunity to work in his team, the weekly group meetings, his advice and his help. Second, I also want to thank George Dadunashvili and Afshin Vahid Belarghou for helping me when needed, especially in improving my programming efficiency. Furthermore, I want to thank the members of the Idema group, for our discussions, their company and their weekly updates on their projects during the group meetings, which gave me a broader knowledge on a variety of biophysical topics.

CONTENTS

INTRODUCTION

1.1. CHEMOTAXIS

Environmental sensing is extremely important in cellular decision making. The sensing allows an organism to observe their external environment, and base their decision making upon it. This makes sensing systems, functioning in a noisy envorinment, an essential network in living organisms. Typically, networks in signal transduction should be robust, only allowing for small errors [2, 3]. Unicellular organisms, like *Dictyostelium Discoidum*, use a combination of membrane-bound receptors and a downstream signalling network which takes input from multiple receptors, to influence the movement of the cell [4]. This process of cellular movement, driven by the chemical gradient in which a cell finds itself is called chemotaxis, and has been studied widely [5–8]. In these studies it is mostly assumed that the outside ligand concentration is known inside the cell as well. The signal transduction fidelity, which is the quality with which the external signal, consisting of receptor activation by ligand binding, is converted into an internal signal with messenger molecules, has been studied less. In this paper we will add to the work of Hille and Dubbeldam [1], whose work consists of analyzing the conversion of the external signal of ligand molecules binding and unbinding, through the cell-membrane, to an internal signal in terms of activated messenger molecules.

The model for transmembrane signal transduction used in this paper is based upon a class of important G-protein coupled receptors in eukaryotic cells. The ligand molecules outside the cell can bind to and unbind from the receptors of the cell, which will activate and deactivate the receptors. Meanwhile the messenger molecules which are diffusing over the membrane, will occasionally pass receptors, and depending on the model that is being used, they will interact with either activated or unactivated receptors. After such an interaction the messenger molecule itself will become activated, carrying the information that a ligand has bound to a receptor. For the most favourable movement, as many bound ligand molecules as possible should be detected by the second messenger system. For this detecting, two opposing mechanisms will be used: 'precoupling' and 'collision coupling' [9, 10].

In this model we use parameter values obtained by studies of the behaviour on cyclic adenosine-monophospate (cAMP) receptors of type 1, (cAR1) in *Dictyostelium Discoidum*, an organism known for its ability to sense chemical concentration gradients with high accuracy [11, 12], even under high thermal and stochastic fluctuations. This makes its signalling system highly suitable for research.

In this paper we extend the models from Dubbeldam and Hille [1], by comparing the precoupling model and collision coupling model in non-homogeneous environments and by reviewing the influence of returning messenger molecules. The results will thus add to the discussion of which of the two mechanisms is the main mechanism for signal transduction in the class GPCRs.

1.2. SECOND MESSENGER SYSTEM

As mentioned before, we will compare two second messenger mechanisms to each other. Both of these mechanisms contain G-protein coupled receptors (GPCRs), which are membrane bound proteins. One of the receptor's ends is outside of the membrane, ligand molecules are able to bind and unbind at this end. The other end, located in the interior of the membrane, is able to react with membrane bound G-proteins $G_{\alpha\beta\gamma}$, the messenger molecules. Upon interacting with the receptor, the messenger molecule will split into two parts: G_α and $G_{\beta\gamma}$, the first of which diffuses in the cytosol, the other will stay membrane-bound. These two subunits are the active parts in the downstream signalling [2, 15–17]. In figure 1 a sketch of both mechanisms can be found.

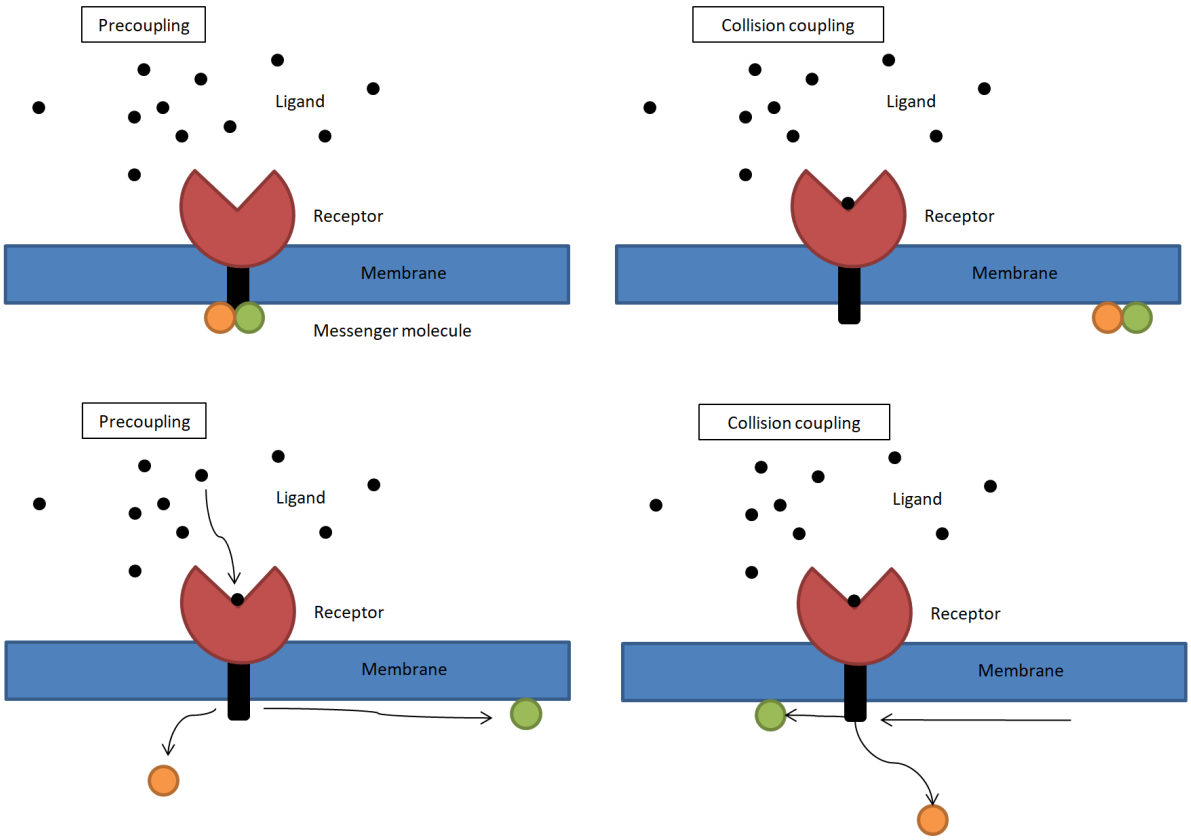

Figure 1: A sketch of the two different mechanisms. On the left, the precoupling mechanism is sketched. First a messenger molecule needs to bind the receptor at the inside of the membrane (top). When a ligand binds the receptor on the outside of the membrane, the messenger molecule splits into its subunits (bottom). On the right, we find the collision coupling mechanism. Here, first a ligand binding a receptor is necessary (top). Now, when a messenger molecule reaches the receptor site, the messenger molecule will split into its subunits (bottom).

One of the two models is the precoupling model. In this model, if a messenger molecule reaches the receptor site of an unbound receptor, it will have a certain chance of coupling to this receptor. After this molecule is coupled to the receptor, no other messenger molecule can interact with this receptor. At the moment a ligand reaches the receptor and binds to it, the messenger molecule will almost immediately react and split in the two subunits. However if no messenger molecule was precoupled to the receptor the moment the ligand reaches the receptor, no detection will be made. During the time that the ligand is bound to the receptor, no messenger molecule can interact with the receptor.

The other model discussed in this paper, is the collision coupling model. Here the messenger molecules will only be able to interact with a bound receptor. If the receptor is unbound, the messenger molecules cannot undergo any interaction with the receptor, however as soon as the receptor binds a ligand, a passing messenger molecule will have a certain probability to interact with the receptor, splitting in the two sub-units.

In figure 2, you can find a visualization of both mechanisms. In these schematics, we use the following abbreviations: R, L, R^* and LR for successively the receptor, the ligand, the precoupled receptor and the ligand-bound receptor.

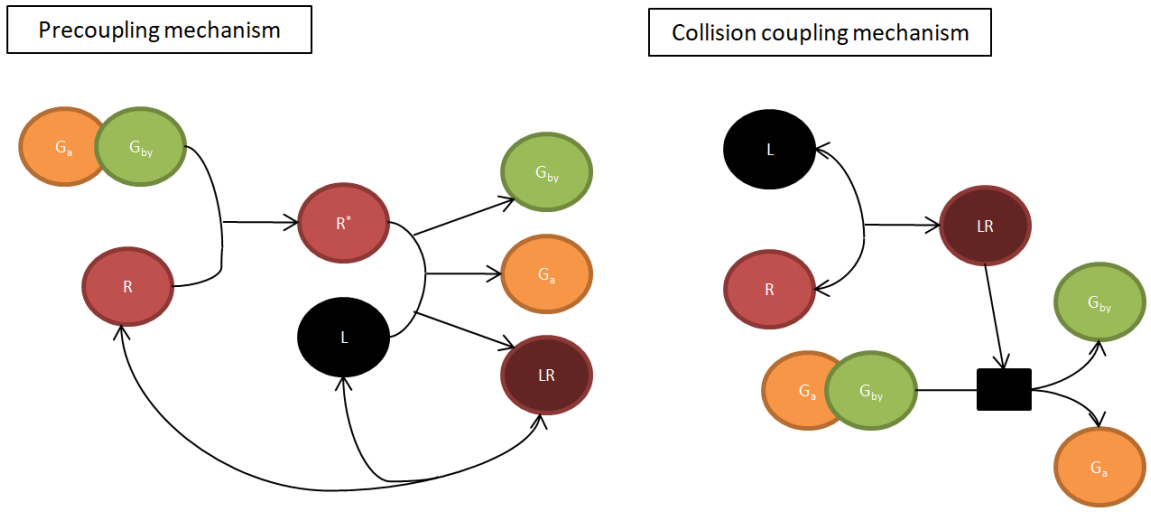

Figure 2: A schematic for both the precoupling and collision coupling mechanism. The black box in the collision coupling mechanism, implies that the LR is not used up in the reaction, but that it's just necessary as a catalyst.

The chemical reactions for the precoupling mechanism in these schematics are:

$$G_\alpha G_{\beta\gamma} + R \rightarrow R^* \tag{1}$$

$$L + R^* \rightarrow LR + G_\alpha + G_{\beta\gamma} \tag{2}$$

$$LR \longleftrightarrow L + R \tag{3}$$

Note that equation 3 states that it is possible for a ligand to bind a receptor that hasn't been precoupled by a messenger molecule, but that this ligand will not be measured.

For the collision coupling we still have equation 3, but now we need to add:

$$LR + G_{\alpha\beta\gamma} \rightarrow LR + G_\alpha + G_{\beta\gamma} \tag{4}$$

In this reaction, LR is a catalyst, which makes the messenger molecule split into its subunits.

A reaction we will add later in both models, is the returning of the messenger molecules. G_α diffuses through the cytosol, and $G_{\beta\gamma}$ diffuses across the membrane, until they find each other and bind again. The rate with which this reaction occurs is so far unknown, but it is guessed to be low.

$$G_\alpha + G_{\beta\gamma} \rightarrow G_{\alpha\beta\gamma} \tag{5}$$

Comparing the two models, some fundamental differences can be found. The most obvious one being that in the precoupling model the messenger molecules can only interact while no ligand is bound to the receptor, on the other hand for the collision coupling model a interaction is only possible while a ligand is bound. This gives the prediction that the precoupling model will be more accurate when little ligand molecules are present, making the typical times of the receptor being unbound large. And that the collision coupling will be more accurate when there is plenty of ligand, because then the receptor will be ligand bounded more often.

Another difference, which is visible in reactions 2 and 4, is the way a messenger molecule splits into its subunits, which is important, since these are the molecules carrying the information of the present ligand molecule. In the precoupling method, a R^* and a L are necessary for a messenger molecule to split, however when reaction 2 takes place, the receptor R^* will lose its precoupled status and bind with the ligand instantly, creating a ligand-bound receptor, which means no second messenger molecule is able to split, creating a maximum of one messenger molecule activation per bound ligand. In the collision coupling case, a bound receptor (LR) is needed for the messenger molecules to get activated. When reaction 4 takes place, this LR is preserved, meaning that if a second messenger molecule arrives at the receptor site before the ligand unbinds the receptor, it is possible that it will get activated as well. No maximum of messenger molecules absorbed per bound ligand is present, except for the trivial maximum which is all the messenger molecules in the system. This raises the expectation that initially the collision coupling model will absorb a lot more of its messenger molecules than the precoupling model. At later times the collision coupling model will have less messenger molecules left, making detecting the binding of new ligand molecules harder, while the precoupling model will have a bigger reserve of messenger molecules.

Both these predictions are also seen in the results of the work of Dubbeldam and Hille.

Numerical Model

2.1. Receptor statistics

Because the numerical model in this report is an extension of the numerical model from Dubbeldam and Hille [1], we will first briefly discuss this model. In this model the activation state of the receptor $R : \mathbb{R}_+ \to \{0,1\}$ follows a periodic pattern, if we take time so that at $t = 0$ the state of the receptor just switched to on, then it will stay on for a given period of time T_{on} (the time it will typically take for a ligand molecule to let go of the receptor), thereafter the state will be switched to off for T_{off} (the time it typically takes for a ligand molecule to bind the receptor).

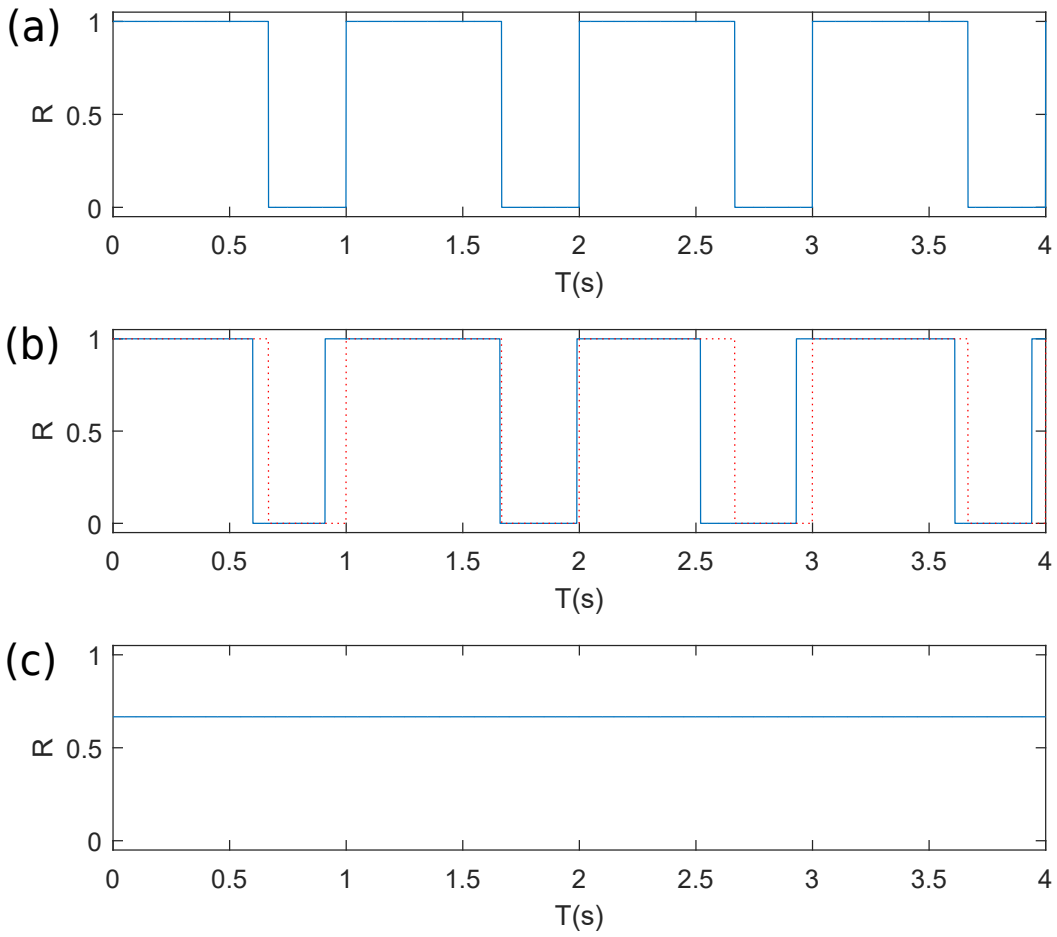

Figure 3: The three different receptor states that will be modeled. The parameters in this model are $T_{\text{on}} = \frac{2}{3}$s, $T_{\text{off}} = \frac{1}{3}$s. (a) The receptor has a fixed periodicity. (b) The state of the receptor is modeled with a Poisson distribution. When the receptor is switched on, the time it will stay on will be randomly chosen via a Poisson distribution with mean T_{on}. When it turns off, the period it will stay off will be randomly chosen by a Poisson distribution with T_{off} as parameter, the dotted line in this figure represents the receptor with a fixed periodicity. In (c) the receptor is always partially on, when a messenger molecule arrives at the receptor site, it has a probability of p of being activated.

This periodicity of the receptor is not something you would expect in reality. A better approximation would be the Poisson distribution. In this model a random time-period will be generated upon the receptor switching its state to on. This random time-period will be generated by a Poisson distribution with mean T_{on}, the receptor will then stay on for this time, after which it will turn off. At this moment, another random time-period will be generated, again by a Poisson distribution, this time with mean T_{off}. Now the receptor state $R : \mathbb{R}_+ \to \{0,1\}$ will turn into a random process, which represents the receptor state used in other research (for example [5, 8]).

In [1] it was found that the ratio of T_{on} to T_{off} was important for deciding which of the two models would be more accurate. That's why in this report we will use a parameter which describes that ratio:

$$p = \frac{T_{on}}{T_{on} + T_{off}} \tag{6}$$

This value of p, together with the parameter $T = T_{on} + T_{off}$, gives us the possibility to model the receptor in a slightly different method. Instead of its state being first on, then off for a certain period of time, it will always be in the same state, it will be on with probability p at all times. The R-function, describing the above will turn into a very straightforward function. $R : \mathbb{R}_+ \rightarrow [0,1]$ can now be described as $R(t) = p$, so R in this model is constant.

All three receptor states discussed above are shown in figure 3.

2.2. Messenger molecules

The messenger molecules (M) are able to move along the entire cell membrane. Although there are multiple receptors on this membrane, in order to keep the model as simple as possible, we will consider just one receptor. To accomplish this, we first divide the membrane up in equal patches, so that each receptor has an equal amount of membrane surrounding it. We assume that the messenger molecules are spread equally, meaning that every patch has one receptor R and an equal amount of messenger molecules M_i (where $i \in \{0, 1, .., N_M\}$, with N_M the number of messenger molecules per patch) in it.

All of these patches will now be simulated as if they are independent of each other. Because the geometry of the system is very simple, a patch can be seen as a bounded domain $\Omega \in \mathbb{R}^2$. All messenger molecules will move trough this domain. There are two areas in this domain worth mentioning: $\Omega_R \in \Omega$, the receptor site and $\delta\Omega$, the boundary of the domain. When a messenger molecule is located somewhere else in the domain, that is: $M \in \Omega/\Omega_R$, it will move uninfluenced by the receptor or other messenger molecules, diffusing freely.

When a messenger molecule reaches $\delta\Omega$, it is about to leave the patch. In this model, another messenger molecule will be randomly placed somewhere else on $\delta\Omega$, this random distribution will be uniform over the entire boundary. This process of relocation over the boundary of the patch, will model the exchange of messenger molecules between the different patches, without changing the total number of messenger molecules per patch. An example of this can be seen in figure 4.

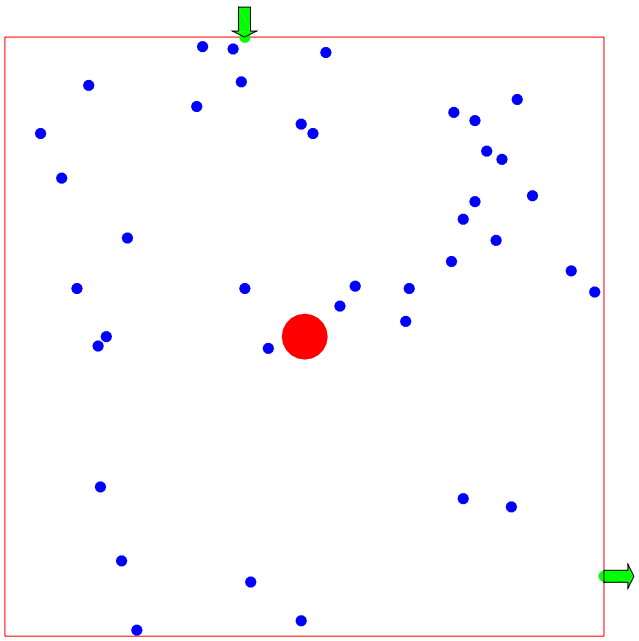

Figure 4: An example of a patch, the moment a messenger molecule leaves the patch (right edge), another messenger molecule will enter (top edge). The location at which the messenger molecules enter, is uniformly chosen over the edge.

The most interesting part of the domain, is Ω_R (the receptor site). When a messenger molecule reaches this receptor site, the molecule will have a certain chance of being absorbed (activated) by the receptor. When a messenger molecule gets absorbed, it gets relocated to the absorbed position, which we will call *. The messenger molecule M_i, whose location will be notated as X_i will thus travel in $\Omega \cup \delta\Omega \cup \{*\}$. The exact probability of a messenger molecule being absorbed depends on which model is being used.

For the collision coupling model, this probability is simple to determine. In the T_{on}, T_{off} model it is just p_{abs}, the absorption chance, while the receptor is in its on state, and 0 while the receptor is in its off state, this is exactly the same for the model with the random switching times. For the T, p model the receptor is always partially on, this means that the probability of absorption will become $p_{abs}p$. This can all be visualized by multiplying all the receptor functions as shown in figure 3 by p_{abs}.

For the precoupling method, determining the probability of a messenger molecule being absorbed will become more complicated. Because a bound messenger molecule will block other messenger molecules from binding, only one messenger molecule can be absorbed per time-period T. This means that in the T_{on}, T_{off} and random switching time models the absorption chance will be p_{abs} from the moment the receptor turns off, until the first absorption is made. It will then be 0 until the receptor switches to its off state the next time. To model this principle of a maximum of one messenger molecules per bound cAMP-particle in the p, T model, we let the probability of activation while at the receptor site be $p_{abs}(1-p)$ initially. As soon as a absorption occurs, this probability is set to 0. Then at $t = mT \ \forall m \in N$. The probability will reset to $p_{abs}(1-p)$, independent of what it was before.

2.3. Quantities for analysis

To analyze the results this model will give, some parameters will be defined. First of all, we will define I_k as the k-th phase of the receptor, one phase during $T = T_{on} + T_{off}$. Which gives us $I_k = [kT; (k+1)T)$. This means that the length of each I_k is the typical time of binding and unbinding of a ligand molecule. To now know if a detection was made during a given I_k, the absorption time T_i for each messenger molecule M_i is introduced. To find T_i we will look for the time that a messenger molecule is placed from Ω_R to *:

$$T_i = \inf\{t > 0 : X_i(t) = *\} \tag{7}$$

Now all that's left is to determine the probability that a detection is made in this I_k, which leads to:

$$A_k = P(\exists i : T_i \in I_k) \tag{8}$$

Physically this means that A_k is the probability for the k-th ligand molecule that binds to be detected by a messenger molecule. Keep in mind that this quantity will only tell us the probability that at least one detection is made in a given time period, it does not give any information about the quantity of the detections during this time period.

The return of messenger molecules from the absorbed state * to $\Omega \cap \delta\Omega$ generally will not be possible, however in section 2.6 the effects of replacing messenger molecules will be looked into.

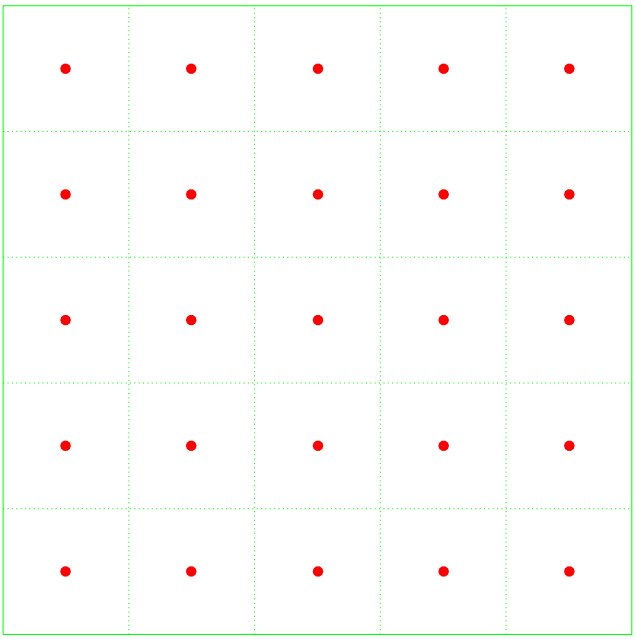

Figure 5: Visual representation of the model used to simulate the influence of patches on each other. Messenger molecules will be able to cross borders separating patches freely, the boundary conditions are periodic. In this visual representation we take $N_R = 25$

2.4. Independent patches

In the first paragraph of section 2.2, it is mentioned that the membrane of the amoeba will be divided into patches, and that all patches will be simulated independently from each other. However a check if this assumption holds up will be done as well. In figure 5 a sketch of the model which will be used for this check is shown. In this model, we will insert N_M messenger molecules per patch in the system and we will let the messenger molecules move back and forth between patches freely. The boundary conditions will be periodic in this model. This way, the conditions for each patch are exactly the same. To make sure that messenger molecules absorbed by different receptors are distinguishable from each other, some more absorbed states are defined. First we will label each patch, starting with R_1 for the patch in the top-left, R_2 for the one next to it (to the right), all the way to R_{N_R} for the receptor in the bottom-right. The different absorbed states will be called $\{*_1, *_2, ..., *_{N_R}\}$ so that a messenger molecule absorbed in R_j will go to $*_j$. In this model, equation 7 and 8 need to be altered slightly so that the information of which receptor absorbed the messenger molecule is included:

$$T_{i,j} = \inf\{t > 0 : X_i(t) = *_j\} \tag{9}$$

$$A_{k,j} = \Pr(\exists i : T_{i,j} \in I_k) \tag{10}$$

Now for any given j, $A_{k,j}$ should have a similar form to A_k in the case where a single patch is simulated.

2.5. Influences across the membrane

The model as described in section 2.4 can also be used for the amount of influence a receptor with different statistics from the receptors in its environment has on those receptors in the environment and vice versa. To accomplish this, one receptor will get a different p-value from the other receptors. Because of the torus-like shape of the system, the receptor that is chosen does not matter for the results. Now suppose R_{j_0} is the receptor with the different p value. A_{k,j_0} will be analyzed and compared to an independently simulated A_k with a receptor which has the same statistics as R_{j_0}. Also for any $j \neq j_0$ a comparison can be made between $A_{k,j}$ and a independently simulated A_k with a receptor with the same characteristics as R_j, it is expected that for this result the distance of R_j to R_{j_0} does not matter, since the diffusion constant is high. This way the

influence of receptors on each other can be seen, however we are also interested in the differences between the different $A_{k,j}$ along the membrane. By comparing A_{k,j_0} to $A_{k.j}$ for $j \neq j_0$ we will be able to see which kind of differences in p along the membrane are notice-able. In [13, 14] we find that in experiments differences as small as 1% across the cell are noticeable.

2.6. Replacing Messenger Molecules

The last addition to the model we are going to introduce is the addition of replacing the messenger molecules back on the membrane. In section 1.2 we have seen that at some point after the activation of a messenger molecule, the G_α will rejoin with the $G_{\beta\gamma}$ and become a messenger molecule again. To model this, we will add a possibility from a messenger molecule M_i with $X_i = *$ to get back to Ω, which was not possible in all other models. We again need to redefine equation 7, first we will define $N : \mathbb{R}_+ \to \mathbb{N}$ as the amount of times a molecule is absorbed before a certain time.

$$N(t) = \#\left[\exists \tau < t : \left[\exists \epsilon > 0 : \forall r < \epsilon : X(\tau) = * \wedge X(\tau - r) \neq *\right]\right] \tag{11}$$

Where the # in equation 11 stands for the amount of times a certain condition is met.

$$T_{i,n} = \inf\{t > 0 : X_i(t) = * \wedge N(t) = n - 1\} \tag{12}$$

So $T_{i,n}$ denotes the n-th time M_i gets absorbed. The placing back of the molecules will be by selecting a random position on $\Omega \cup \delta\Omega$ at $t = T_{i,n} + T_r$, where T_r is the time of replacement. Now the equivalent equation to equation 8 will be:

$$A_k = \Pr(\exists i, n : T_{i,n} \in I_k) \tag{13}$$

ANALYTICS

3.1. EXPRESSIONS FOR DETECTING PROBABILITIES

In the following section, we will discuss A_k from a probabilistic perspective. The expressions we will get this way, should help us understand the behaviour of A_k when changing the values of p or k. In section 4, we will compare this expected behaviour to the behaviour we see in the simulations.

Collision Coupling

To determine the receptor signal of the collision coupling model analytically, we need to know what the probability is for a given k that at least one messenger molecule is absorbed in I_k, the k-th phase, by basic probability theorems we find an alternate form for equation 8:

$$A_k = 1 - \mathrm{P}(\forall i : T_i \notin I_k)$$

Which, by realizing that all M_i are independent of each other, can be rewritten as:

$$A_k = 1 - (1 - P(T_i \in I_k))^{\mathrm{N_M}} \tag{14}$$

Now we see that to determine A_k we only need to calculate $P(T_i \in I_k)$. We regard the entire patch as one trap, where the total probability of being absorbed will be determined by multiplying its 3 components: The probability that the messenger molecule is in the receptor: $\frac{\mathrm{A_{rec}}}{\mathrm{A_{patch}}}$, the probability that the receptor is ligand-bound: p, and the absorption probability: p_{abs}.

We use a discrete model, where each I_k consists of $\mathrm{N_T}$ time units (the chosen time units are motivated by the diffusion constant of the messenger molecules). Therefore we find that for the first phase, by the same probability theorems as before, $\mathrm{P}(T_i \in I_k)$ becomes the probability that the messenger molecule does not survive all time units of one phase, which we will call b:

$$b(p) = 1 - \left(1 - \mathrm{p_{abs}} p \frac{\mathrm{A_{rec}}}{\mathrm{A_{patch}}}\right)^{\mathrm{N_T}} \tag{15}$$

For any later phase, the messenger molecule must first survive all previous k-1 phases, and given that it has survived those first k-1 phases, the probability that it will get absorbed in the k-th phase is the same as the probability of the messenger molecule getting absorbed in the first phase initially was, this gives us:

$$P(T_i \in I_k) = b\left(1 - \sum_{j=1}^{k-1} P(T_i \in I_j)\right) \tag{16}$$

Equations 14, 15 and 16 give an analytic expression for A_k by themselves, however by further analyzing 16 we find that it can be rewritten as equation 17. A proof that equation 16 and 17 are equal can be found in appendix A.

$$P(T_i \in I_k) = b(1-b)^{k-1} \tag{17}$$

In the appendix, we show by induction that equation 16 is always equal to the binomial expansion of 17. Using this result we find the following expression for A_k:

$$A_k = 1 - (1 - b(p)(1 - b(p))^{k-1})^{\mathrm{N_M}} \tag{18}$$

In this equation we find that A_k is only dependent on b, which is a function of p, p_{abs}, $\mathrm{A_{rec}}$, $\mathrm{A_{patch}}$ and $\mathrm{N_T}$, however we will assume all those variables constant except for p. In figure 6 we plot equation 18 for $p = 0.5$.

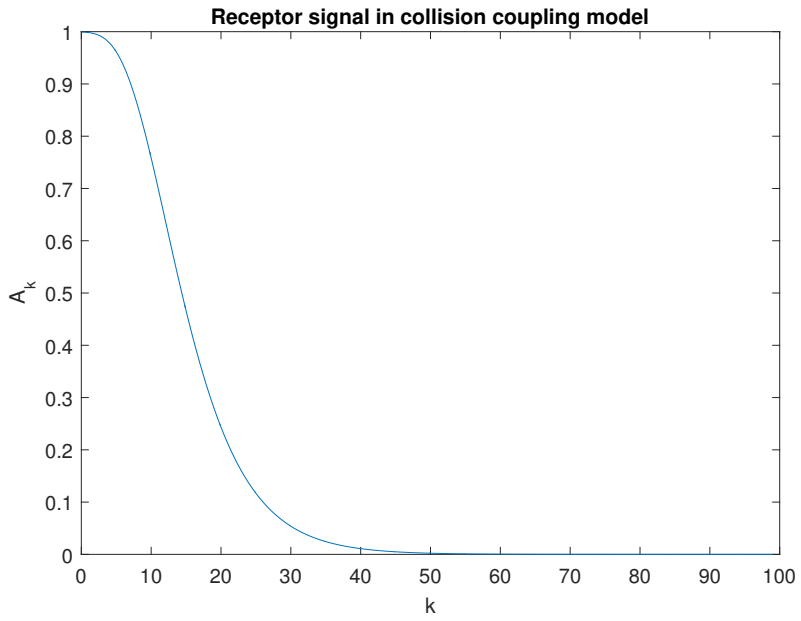

Figure 6: The expected receptor signal for $p = 0.5$, parameters used cam be found in table 1 in section 4

Precoupling

For the precoupling model we will follow a different strategy. First we define a variable which is only dependent on p, similarly to the collision coupling model:

$$b(p) = \left(1 - p_{\text{abs}}(1-p)\frac{\text{A}_{\text{rec}}}{\text{A}_{\text{patch}}}\right)^{\text{N}_\text{T}} \tag{19}$$

Now if at the start of phase k^* we have n active messenger molecules we will have:

$$A_{k^*} = 1 - b^n \tag{20}$$

So the only problem that remains is determining how many messenger molecules are on average active for a given k. For $k = 1$, we can fill in $n = \text{N}_\text{M}$ in equation 20 to get A_1, since we start with N_M messenger molecules. Now because a maximum of one M gets absorbed in the first phase, we will have a probability of A_1 that there are $\text{N}_\text{M} - 1$ messenger molecules left, and a probability of $1 - A_1$ that still N_M are left. This results in:

$$A_2 = A_1(1 - b^{\text{N}_\text{M}-1}) + (1 - A_1)(1 - b^{\text{N}_\text{M}}) \tag{21}$$

We continue for A_3, now there is a probability of $A_1 A_2$ that 2 messenger molecules are absorbed, there are two possibilities that 1 M gets absorbed: It gets absorbed in I_1 or it gets absorbed in I_2, resulting in a probability of $A_1(1 - A_2) + (1 - A_1)A_2$. The probability that no M get absorbed will be $(1 - A_1)(1 - A_2)$. Giving us the following expression:

$$A_3 = A_1 A_2(1 - b^{\text{N}_\text{M}-2}) + (A_1(1 - A_2) + (1 - A_1)A_2)(1 - b^{\text{N}_\text{M}-1}) + (1 - A_1)(1 - A_2)(1 - b^{\text{N}_\text{M}}) \tag{22}$$

A pattern emerges! In general we have:

$$A_k = \sum_{i=0}^{k-1} B_{k,i}(1 - b^{\text{N}_\text{M}-(k-1)+i}) \tag{23}$$

Where $B_{k,i}$ is the probability that $(k-1)-i$ absorptions have taken place, after $k-1$ phases. This factor depends on $A_1, A_2, ...A_{k-1}$, and defined for $k \in \mathbb{N}$ and $i = 0, 1, ..., k-1$. An expression for this factor:

$$B_{k,i} = \sum_{j_1=1}^{k-i+1} \sum_{j_2=j_1+1}^{k-i+2} ... \sum_{j_{i-1}=j_{i-2}+1}^{k-1} \left(\prod_{l=1}^{k-1} A_l \right) \frac{(1-A_{j_1})(1-A_{j_2})...(1-A_{j_{i-1}})}{A_{j_1} A_{j_2} ... A_{j_{i-1}}} \tag{24}$$

The total amount of sums in equation 24 is $i-1$, the equation gives the total probability of all possible combinations of $(k-1)-i$ molecules getting absorbed combined, thus it is the probability that the system has $N_M - (k-1) + i$ messenger molecules at the start of I_k.

Combining $A_1 = 1 - b^{N_M}$ with equation 19, 23 and 24 gives us an analytic expression for what will be simulated. Unfortunately, the expressions are not very practical and do not help us with analyzing behaviour of the receptor signal for the precoupling model.

3.2. Stealing particles

In section 2.5 the model in which multiple connected patches are simulated is introduced. Here all but one patch have receptors with identical p-values, the patch that has a receptor with a different p-value will be called R_{in}, all other patches will be referred to as R_{out}. What will happen in this model, is that the patches will exchange messenger molecules. However, if a patch has a receptor with a higher p-value than its neighbours, it will generally have less messenger molecules leaving the patch, than entering it. This is because it will absorb more of its messenger molecules, thus leaving less of them to leave the patch. Effectively it is stealing messenger molecules from its neighbours. That is, more messenger molecules will be absorbed into the receptor with the higher p-value than the N_M that originally were inserted into that patch, on the other hand, its neighbours will absorb slightly less messenger molecules than those initial N_M. We define the following set of parameters:

$$\begin{aligned} p_{in} &= p_{in} p_{abs} \frac{A_{rec}}{A_{patch}} \\ p_{out} &= p_{out} p_{abs} \frac{A_{rec}}{A_{patch}} \\ B_{in} &= \frac{4}{\sqrt{A_{patch}}} \\ B_{out} &= \frac{4}{\#R_{out}\sqrt{A_{patch}}} \end{aligned}$$

Here p_{in} denotes the p-value of R_{in}, while p_{out} is the p-value of all other receptors R_{out}. We write $\#R_{out}$ for the amount of receptors R_{out}. Physically, the meaning of the variables are respectively: The probability of a messenger molecule getting absorbed while in the patch with R_{in}, the chance of an absorption while in any other patch, the probability for a messenger molecule to go away from the patch with R_{in}, the probability to get into the patch with R_{in}. In figure 7 a visual representation of the parameters is added.

The main thing we are interested in is the amount of messenger molecules absorbed per receptor, when starting with a uniform distribution over the entire membrane. This will give us an idea of the influence receptors have on each other.

Because of the different absorption mechanisms of the precoupling and the collision coupling model, both models will be treated separately.

Collision coupling

With the definitions in the table at the top of this page, we can set up a set of differential equations for $n_{in,act}$ the amount of active messenger molecules inside the patch with receptor R_{in}, and $n_{out,act}$ for the amount of messenger molecules outside this patch:

$$\frac{dn_{in,act}}{dt} = -(p_{in} + B_{in})n_{in,act} + B_{out} n_{out,act} \tag{25}$$

$$\frac{dn_{out,act}}{dt} = -(p_{out} + B_{out})n_{out,act} + B_{in} n_{in,act} \tag{26}$$

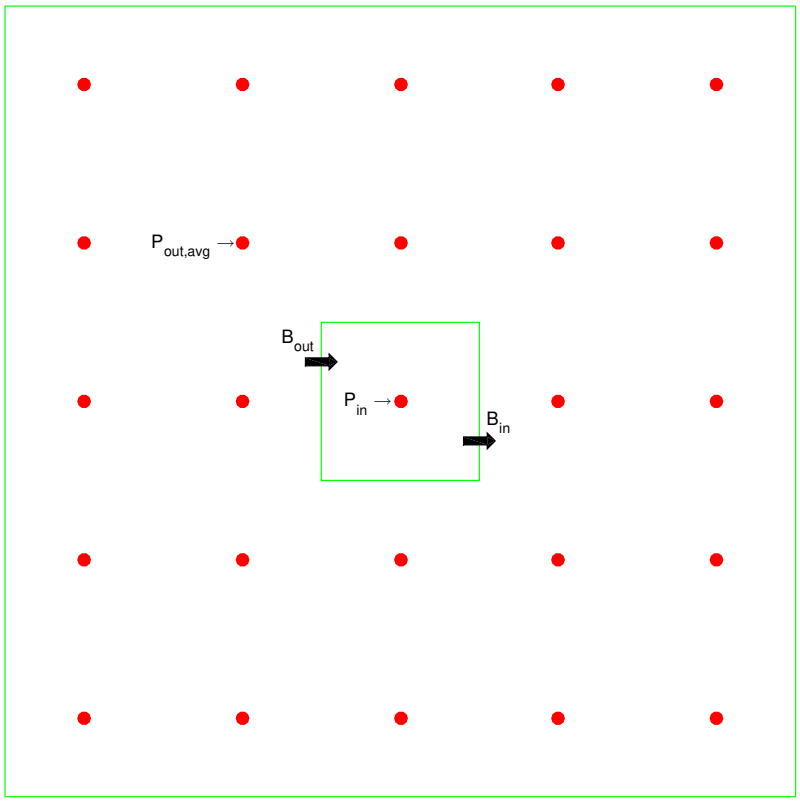

Figure 7: Visual representation of the parameters defined for the differential equations to model the absorption of messenger molecules and the exchange of the messenger molecules between patches. The P variables picture the probability of absorption when in the patch with that receptor. B_{in} is the probability of leaving the patch with the receptor with P_{in} when in that patch, B_{out} is the probability of entering that patch when not in it.

Equation 25 and 26 model the change in the amount of messenger molecules due to crossing the border or getting absorbed both in and out of the special patch. To remember how many of the messenger molecules get absorbed inside R_{in} we introduce $n_{in,abs}$, $n_{out,abs}$ will be used for messenger molecules absorbed in any of the other receptors.

$$\frac{dn_{in,abs}}{dt} = p_{in} n_{in,act} \tag{27}$$

$$\frac{dn_{out,abs}}{dt} = \frac{p_{out}}{N_R - 1} n_{out,act} \tag{28}$$

In equation 28 we average out over all receptors, so that we will get the amount of messenger molecules that typically get absorbed in one R_{out}. Now since equation 25, 26, 27 and 28 are all linear, they can be written in matrix form. However, since equation 27 and 28 are not independent from the other two, they are not included in the matrix.

$$\begin{bmatrix} \frac{dn_{in,act}}{dt} \\ \frac{dn_{out,act}}{dt} \end{bmatrix} = \begin{bmatrix} -(p_{in} + B_{in}) & B_{out} \\ B_{in} & -(p_{out} + B_{out}) \end{bmatrix} \begin{bmatrix} n_{in,act} \\ n_{out,act} \end{bmatrix} \tag{29}$$

As initial conditions, we will add N_M messenger molecules per patch:

$$\begin{bmatrix} n_{in,act}(0) \\ n_{out,act}(0) \end{bmatrix} = \begin{bmatrix} N_M \\ (N_R - 1)N_M \end{bmatrix} \tag{30}$$

Such a matrix equation can be solved analytically. The solution is plotted in figure 8(a).

Precoupling model

The border crossing probabilities, B_{in} and B_{out} only depend on the size of a patch, so they do not change when we change models. The absorbing probabilities however do change. To calculate the amount of messenger molecules that will get absorbed per time unit, $\dot{n}_{in,abs}$ and $\dot{n}_{out,abs}$, we realize that over one k-phase the total amount of messenger molecules absorbed should be equal to the probability a single messenger molecule getting absorbed, since after this one molecule is absorbed, it will block the receptor for further absorptions. So we will calculate the total chance of a messenger molecule getting absorbed in one k-phase, then spread this out equally over all time units of this phase, resulting in:

$$\frac{dn_{in,abs}}{dt} = \frac{1-\left(1-p_{abs}(1-p_{in})\frac{A_{rec}}{A_{patch}}\right)^{n_{in,act}N_T}}{N_T} \tag{31}$$

We follow this routine for all other receptors:

$$\frac{dn_{out,abs}}{dt} = \frac{\#R_{out}\left(1-\left(1-p_{abs}(1-p_{out})\frac{A_{rec}}{A_{patch}}\right)^{\frac{n_{out,act}}{N_R-1}N_T}\right)}{N_T} \tag{32}$$

Now the change in active molecules in the patch with R_{in} is just adding the amount of molecules entering the patch and subtracting those leaving and those getting absorbed. The same analysis holds for the other receptors. This leads to the following differential equations:

$$\frac{dn_{in,act}}{dt} = -\frac{1-\left(p_{abs}(1-p_{in})\frac{A_{rec}}{A_{patch}}\right)^{n_{in,act}T}}{T} - B_{in}n_{in,act} + B_{out}n_{out,act} \tag{33}$$

$$\frac{dn_{out,act}}{dt} = -\frac{\#R_{out}\left(1-\left(p_{abs}(1-p_{out})\frac{A_{rec}}{A_{patch}}\right)^{\frac{n_{out,act}}{\#R_{out}}T}\right)}{T} - B_{out}n_{out,act} + B_{in}n_{in,act} \tag{34}$$

In contrary to the collision coupling case, unfortunately the set of differential equations we obtained for the precoupling model is not linear, the equations can only be solved numerically. The solution is plotted in figure 8(b).

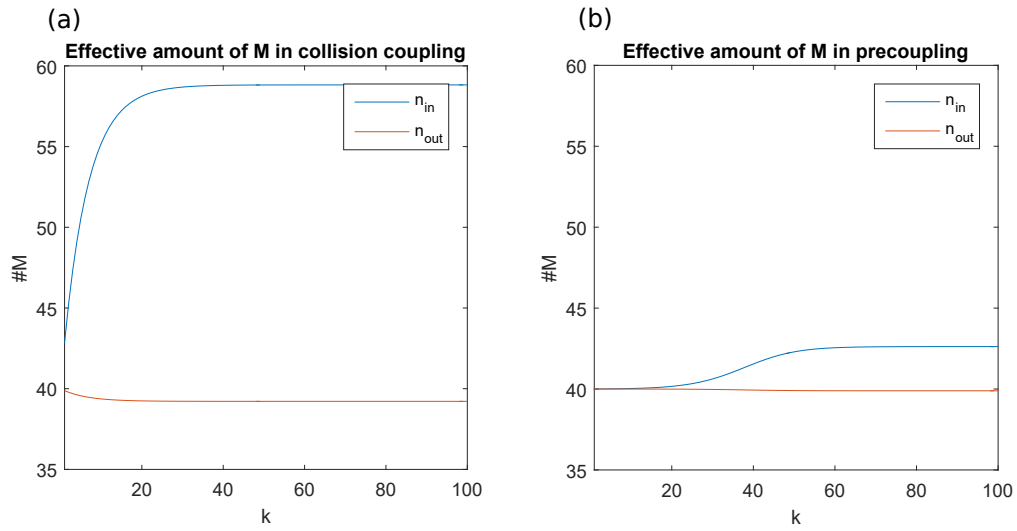

Figure 8: The amount of M in R_{in} and the average amount of M per R_{out} are shown for the first 100 k-phases. In (a) the results for the collision coupling model can be seen and in (b) the results for the precoupling model are shown. The values for the parameters used can be found in table 1 in section 4, further we used $p_{in} = 0.75$ and $p_{out} = 0.5$ for the collision coupling model and $p_{in} = 0.33$ and $p_{out} = 0.5$ for the precoupling model.

In figure 8 we see the solution of the two sets of differential equations. Here we plot the total amount of messenger molecules inside and outside the patch ($n_{in} = n_{in,act} + n_{in,abs}, n_{out} = n_{out,act} + n_{out,abs}$). A further analysis on these solutions can be found in section 4.4.

3.3. Long term limits in the replace-rate model

For the messenger molecule replace model (as described in section 2.6), messenger molecules will constantly leave and re-enter the system. This will happen until an equilibrium is found. In this section we will look for this equilibrium. The two models are again treated separately.

Collision coupling model

For the amount of molecules that get absorbed per time-unit we find:

$$M_- = p_{abs} p \frac{A_{rec}}{A_{patch}} n \tag{35}$$

Where n is the amount of active messenger molecules. For the amount of messenger molecules coming back on the patch per time-unit we have:

$$M_+ = \frac{N_M - n}{T_r N_T} \tag{36}$$

Where T_r is the amount of phases I_k between absorption and replacement of a messenger molecule. An equilibrium is settled when $M_- = M_+$, which gives us the following expression for the amount of active messenger molecules at equilibrium:

$$n_e = \frac{N_M}{T_r N_T p_{abs} p \frac{A_{rec}}{A_{patch}} + 1} \tag{37}$$

Per I_k, a total of $N_T p_{abs} p \frac{A_{rec}}{A_{patch}} x$ messenger molecules will get absorbed when there are x molecules present in the system, so the amount of k-phases it will take for the first $N_M - n_e$ to get absorbed is:

$$k_e = \frac{1}{N_T p_{abs} p \frac{A_{rec}}{A_{patch}}} \int_{n_e}^{N_M} \frac{1}{x} dx \tag{38}$$

After simplifying equation 38 and using our results from equation 37, we find:

$$k_e = \frac{1}{N_T p_{abs} p \frac{A_{rec}}{A_{patch}}} \ln\left(T_r N_T p_{abs} p \frac{A_{rec}}{A_{patch}} + 1\right) \tag{39}$$

Using this k_e in equation 18 will give us a prediction to the value of A_{k_e} we would get in the long term limit.

Precoupling model

In the precoupling model, we follow the same procedure. First we calculate the average amount of messenger molecules getting absorbed in one phase, given that there are n messenger molecules left in the patch. Since it's not possible in the precoupling model for more than one messenger molecule to get absorbed per phase. This average amount of messengers absorbed will be equal to probability of one messenger getting absorbed in a phase given that n messenger molecules are left. This probability will be spread out over all the time units of such a phase:

$$M_- = \frac{(1 - p_{abs}(1-p)\frac{A_{rec}}{A_{patch}})^{nT}}{N_T} \tag{40}$$

The way in which messenger molecules are replaced, does not change with the model being used, equation 36 is still valid here, again we continue by putting $M_- = M_+$ to get n_e, however due to the term n appearing both linearly and exponentially, this time an analytic expression cannot be found. We advance with the numerical result for n_e. Similar to equation 39 we calculate the amount of phases this usually takes in the model without replacements. In the precoupling model, since the integral of A_k from 0 to k^* is the amount of absorbed messenger molecules in the first k^* phases, we need the following infimum:

$$k_e = \inf\left\{k : \int_0^k A_x dx \geq N_M - n_e\right\} \tag{41}$$

Using found k_e in the equations found in the precoupling section of section 3.1 will give us an approximation for the equilibrium value A_{k_e}.

SIMULATION RESULTS

In this section we will use the following numerical values for earlier introduced parameters for the amount of time units per k-phase, the amount of messenger molecules, the area of the receptor, the area of the patch and the absorption probability:

Table 1: Simulation Parameters

Parameter	N_T	N_M	A_{rec}	A_{patch}	p_{abs}
Value	200000 t_u	40	1 nm^2	40000 nm^2	0.06453

The t_u in table 1 denotes the time unit in our model, which is chosen to be the average time it takes for a messenger molecule to diffuse 1 nm^2. With $D = 1.5 * 10^5 \frac{nm^2}{s}$ we find 1 $t_u = 3.3 * 10^{-6}$s. Each k-phase will take 200000 $t_u = 0.67$ s. [18]

The size of the patch we are going to analyze is 200nm by 200nm with a receptor of 1 nm^2 in the middle. The patch will have 40 messenger molecules, the value of p_{abs} is motivated by the binding rate of a messenger molecule to a receptor and the time units used. [1]

4.1. P-VALUES

Collision Coupling Model

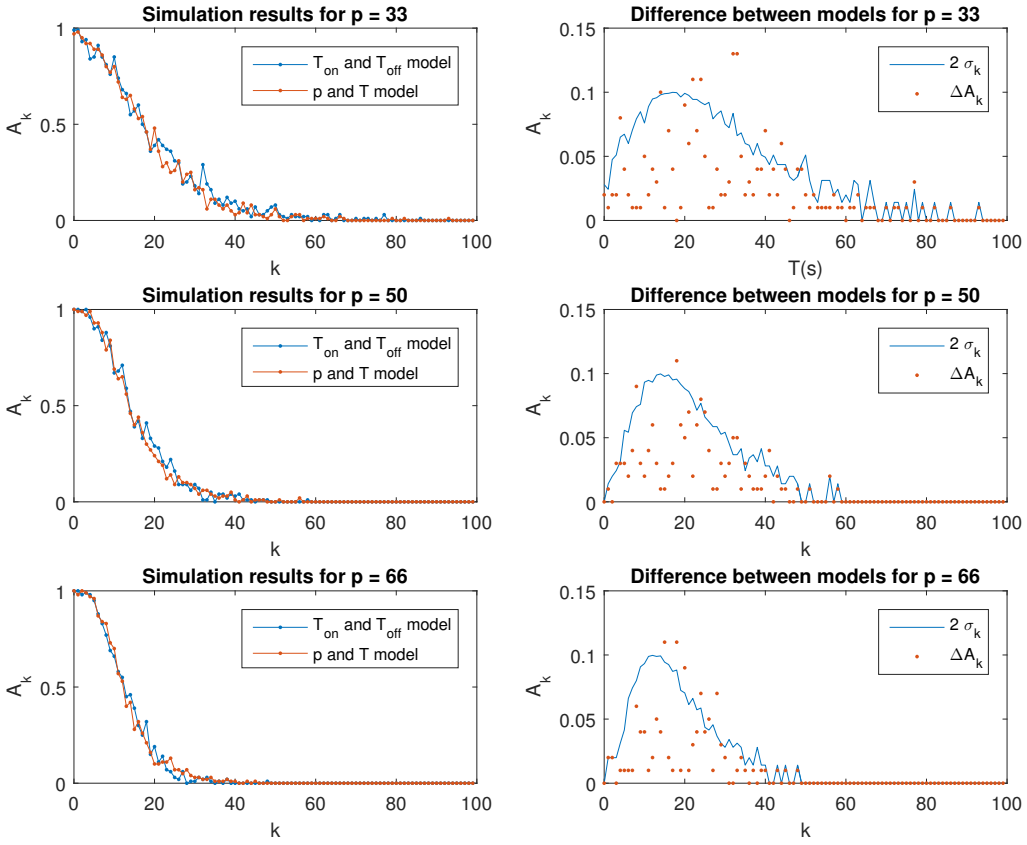

Figure 9: Comparison between the model using T_{on} and T_{off} as parameters and the model using p and T as parameters for the collision coupling model. The corresponding values for T_{on} and T_{off} can be calculated by $T_{on} = pT$ and $T_{off} = (1-p)T$. On the left the results for both models are displayed, on the right the differences between the model and the standard deviation of the data are shown.

Because the T_{on} and T_{off} variables from the model in [1] got replaced by T and p, we will first check the assumption that changing those variables would not have an impact on A_k. In the left half of figure 9, the results of simulation using both models are shown. In the right half of the figure it is shown that the difference of the value of A_k produced by the different models is almost always smaller than two standard deviations. The standard deviations in this figure are calculated by:

$$\sigma_k = \sqrt{\frac{A_k(1-A_k)}{N}} \tag{42}$$

This standard deviation is calculated independently for every k. The N in equation 42 is the number of runs used in the simulation of the data. Every data point for A_k is interpretable as a Bernoulli variable; in a single run, the k-th event of binding is either detected or undetected, so equation 42 is simply the standard deviation of a Bernoulli variable after N tries. The value for A_k used in this equation is the average value of the T_{on}, T_{off} and P, t model. We find that for 90% of the data-points, the difference between the results for A_k in the models is below 2 standard deviations. Given these results, the swap of variables is acceptable for the collision coupling case.

Precoupling Model

For the precoupling model, exactly the same is done as for the collision coupling model, both the T_{on}, T_{off} and the T, p variants of the model are used for simulations and the results again will be compared in figure 10. In this figure we have σ_k defined the same way as before (equation 42). Again, the differences between the results seem to be due to chance rather than method. The difference between the two results for A_k is smaller than 2 standard deviations for 85% of the data, also making the swap of variables acceptable for the precoupling model.

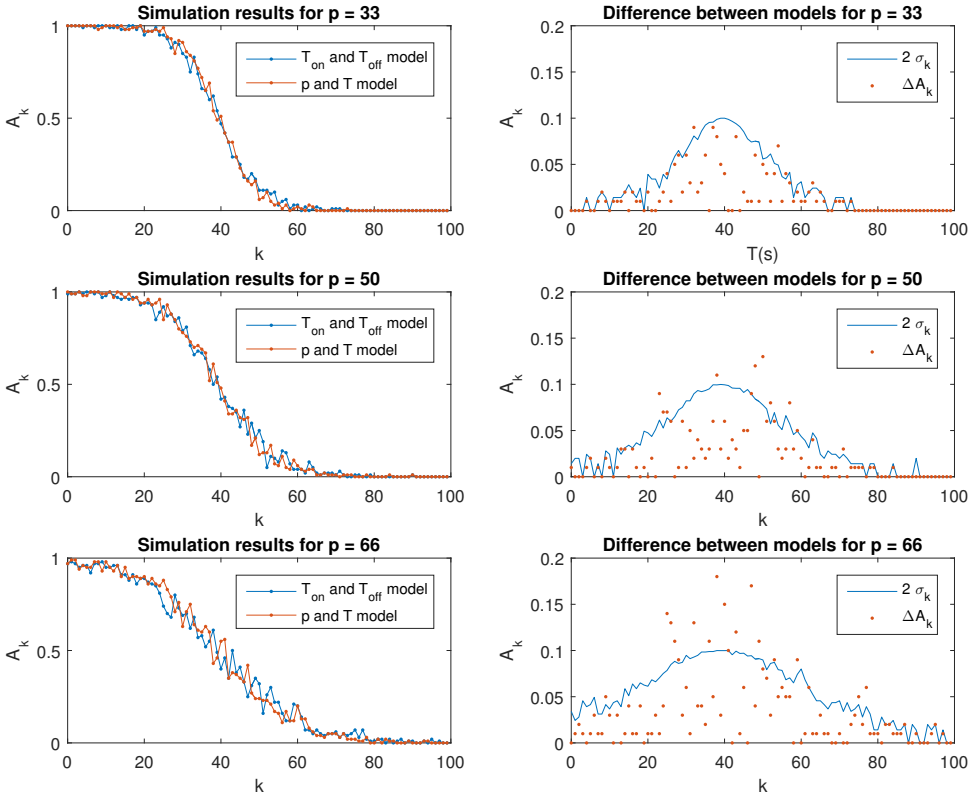

Figure 10: Comparison between the model using T_{on} and T_{off} as parameter and the model using p and T as parameter for the precoupling model. The corresponding values for T_{on} and T_{off} can be calculated by $T_{on} = pT$ and $T_{off} = (1-p)T$. On the left the results for both models are displayed, on the right the differences between the model and the standard deviation of the data are shown.

4.2. Poisson distributed on and off times

Implementing Poisson distributed switching times for the receptor instead of a periodic receptor with static on and off times did not have a significant impact on A_k, the figures containing the results of this section can be found in appendix B. For all generated data points only 14 % had a difference larger than 2 standard deviations using the precoupling model, and only 11% using the collision coupling model. If we compare this to two different sets of runs, generated with the same model, still 13% of the data-points are further apart than 2 standard deviations. The little difference between fixed switching times and switching times chosen via a Poisson distribution tells us that the simple model of choosing fixed switching times is sufficient for determining the receptor signal.

Since the assumption that the differences in A_k are small when switching between the 3 receptor functions described in section 2.1 holds up, we will continue with the p, T-versions of the models.

4.3. Scaling

Upon analyzing the results in figure 9 all three A_k-curves seem to have a similar shape, which raises hope for the possibility of a scalable k-axis. The same can be said for the different plots in figure 10. The importance of this scaling is that once we find a way of scaling the k-axis, we can disregard the p-value of the receptors and just do simulations for one p-value.

Note that for the collision coupling model we already found an expression that should describe the data. The problem with this equation is that the k-parameter and the free p-parameter have an exponential relation, so that it isn't suitable for scaling.

Collision Coupling

An expression that represents the results of A_k (motivated by the data following a Gaussian decaying shape):

$$A(k) = \exp\left(-\left(\frac{k}{c}\right)^2\right) \tag{43}$$

In figure 11 the best fit for equation 43 is shown for 8 different p values:

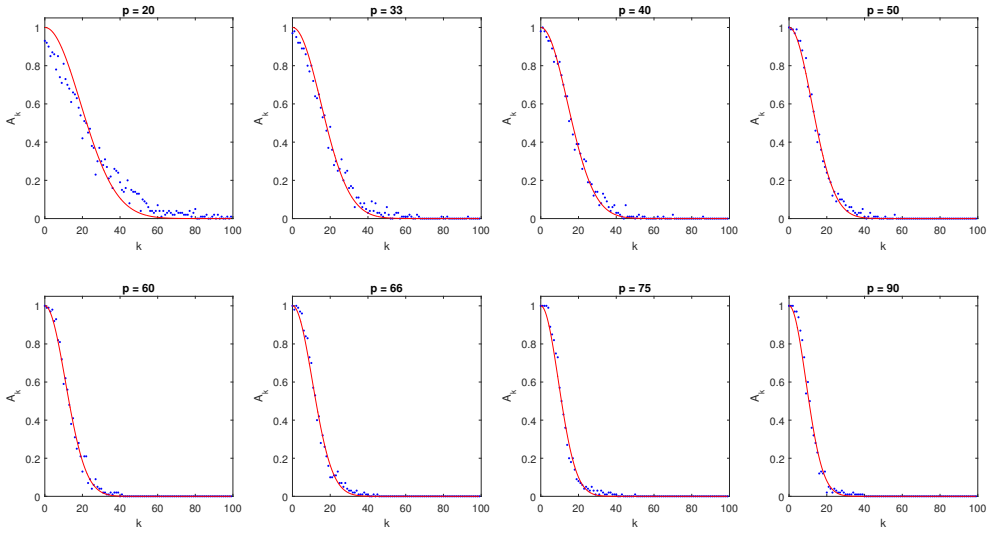

Figure 11: Fit of equation 43 to simulated data for various values of p, simulated data is generated with the collision coupling model.

With the exception of the $p = 20$ simulation, the fit seems to perform well. However small details get lost with this fit, one of those details being for $k \leq 4$. Here, the fit is forced to start at one and then move away from it

exponentially, however for low p it was seen that in the simulations, the first ligand was not detected with a 100% accuracy, and for high p the exponential of A_k does not start immediately. Another detail which misses in the fits is in the region that $0.02 < A_k < 0.15$, here the fits will typically sustain the decay they had in the region before $A_k < 0.15$, however the simulated data shows that the decay slowed down more.

Although the fit is not perfect, it will work for the goal we have: finding a scaling parameter. In figure 12(a) the fitting parameter c from equation 43 is plotted against the p-value of the receptor, in this plot, error bars with the size of a standard deviation are added as well.

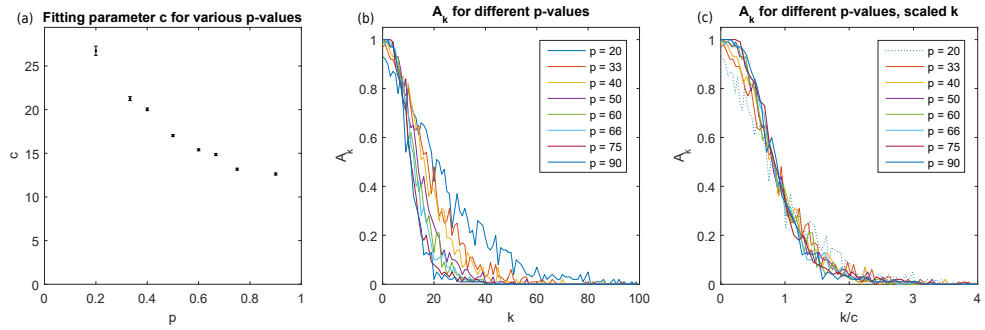

Figure 12: Scaling in the collision coupling model, in (a) the best fit-parameter to equation 43 is shown for different p-values. In (b) the simulation results are shown for different p-values and (c) shows the same results, after scaling the k-axis with the c corresponding to the used p-value.

In figure 12(b) the graphs of A_k are shown for all different p-values shown in figure 11, before scaling k, figure 12(c) shows what happens after this scaling, the graphs of the different A_k now overlap, in this figure, the line for $p = 20$ is dotted, because the fit for this value was not good, which means that in that region the approximation of A_k with equation 43 might not be valid.

The simulations showed that for $p \geq 0.33$, A_k will look the same after scaling the k-axis with a parameter which depends on p, a question rises: Can this dependency be explained? In figure 12(a) it is clear that c drops when p rises. To explain this we will look at the analytically derived equation of A_k (14) with $\frac{k}{c}$ instead of k. b rises as p rises (equation 15). We see that for $k > 1$, $\mathrm{P}(T \in I_k)$ decreases with increasing p, and with increasing k (equation 17). By increasing c we decrease $\frac{k}{c}$, so that this decrease and the increase of p together will cancel each others effects for $\mathrm{P}(T \in I_{\frac{k}{c}})$, resulting in the same A_k.

The exact relation between p and c isn't clear, a best guess can be made:

$$c(p) = \frac{a}{p} + b, \text{ with } a = 3.7 \pm 0.4 \text{ and } b = 9 \pm 1 \tag{44}$$

The analytic equation 18 we found in section 3.1, should approximate the simulated data even better. A fit of the same simulation data as in figure 11 to this equation is shown in figure 13.

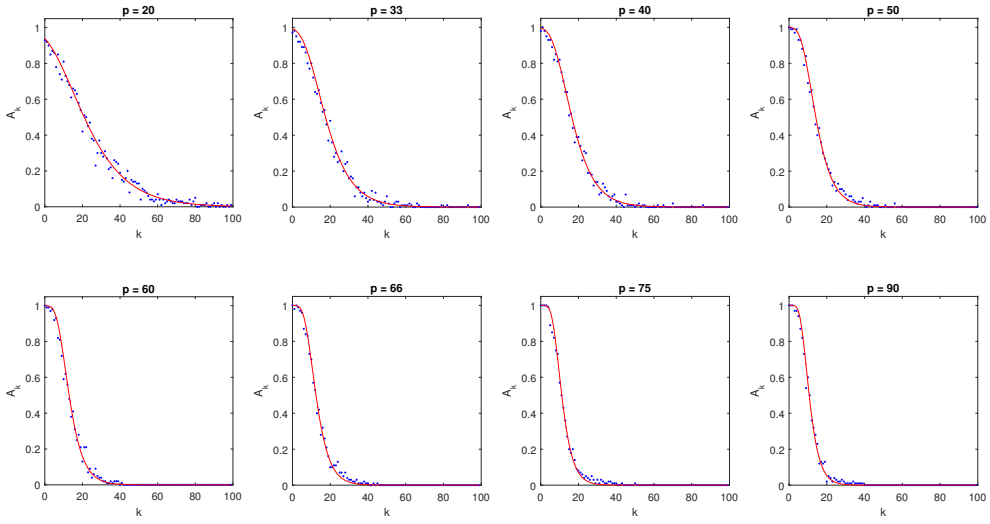

Figure 13: Best fit of equation 18 to simulated data, generated with the collision coupling model.

Here we see that for every p-value a good-performing fit to equation 18 can be found. Furthermore, this fit produces a measured value for p: the p used in equation 18 which yields the best fit for the simulated data. This measured p will be compared to the p used in the simulations in figure 14.

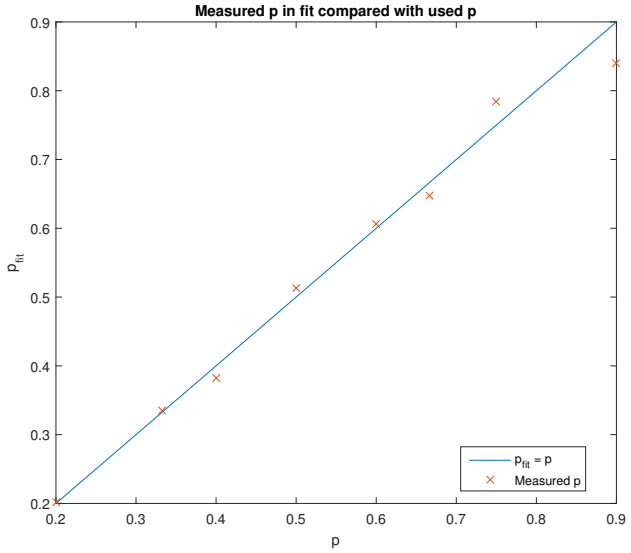

Figure 14: A comparison between the best fit of p to equation 18 and the p-value used to simulate the data.

In this comparison, we see that, especially for low p the measured and used p are close to equal. For higher p the errors get higher, but they never exceed 7%. This tells us that the analytic model from section 3.1 for the collision coupling mechanism does indeed model the collision coupling mechanism very accurately.

The reason for the higher errors for high p is that effectively less data is available, since more messenger molecules get absorbed per k-phase, resulting in less nonzero data-points.

Fundamentally the analytic expression 14 and the scaling fit 43 should behave differently. To look into the differences, a comparison of the two has been added in appendix C.

Precoupling

In figure 10 we see that A_k for the precoupling model all follow a general pattern as well, this pattern is different from the pattern in the collision coupling model. It consists of staying close to 1 for the first few k, then decreasing exponentially around $k = 40$ until it gets close to 0. Depending on the p-value of the receptor, both the amount of k-phases it stays 'close' to 1 and the rate of increasing change, however these two events are correlated. We compare the simulation results to the following equation (motivated by [19]):

$$A(k) = \frac{1}{1 + \exp(\frac{k - \mathrm{N_M}}{c})} \tag{45}$$

In this equation the term $\exp(\frac{k}{c})$ in the enumerator determines the rate of decay, while the $\exp(-\frac{\mathrm{N_M}}{c})$ term accounts for the amount of k-phases that $A(k)$ stays close to 1.

Note that in equation 45 $A(\mathrm{N_M}) = 0.5$ always holds, which won't be true in general. For $p \to 1$ the probability of the receptor being in its off state becomes small, which makes the chance of a messenger molecule precoupling small. Simple evaluation of equation 20 shows that for $p \geq 0.95$, $A_1 < 0.5$, A_k is a monotone decreasing function so for p-values above 0.95 the condition $A(\mathrm{N_M}) = 0.5$ will never hold. However for the largest part of the domain we are interested in, this condition held up. Further analysis on this equation shows that it integrates to:

$$I = c \log\left(e^{\frac{\mathrm{N_M}}{c}} + 1\right) \tag{46}$$

In this expression, I should be equal to the total amount of messenger molecules $\mathrm{N_M}$. Again, in general this is not true, however as long as $\frac{\mathrm{N_M}}{c}$ stays big, the equation will approximate $\mathrm{N_M}$. For $\frac{\mathrm{N_M}}{c} \geq 4$ the difference between $\mathrm{N_M}$ and I will not be more than 2%.

In figure 15, the simulation data is shown, together with the best fit of equation 45 to this data.

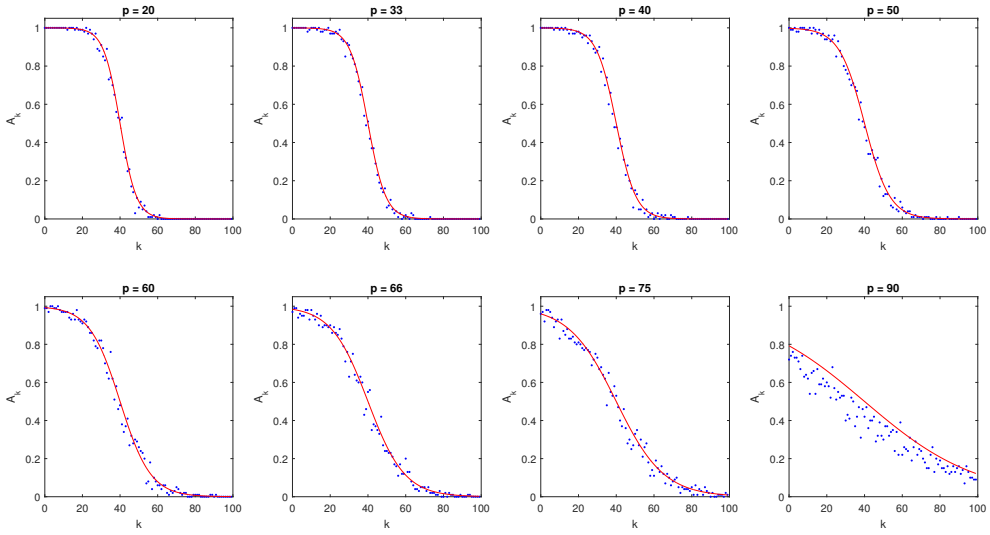

Figure 15: Fit of equation 43 to simulated data for various values of p, simulated data is generated with the precoupling model.

As with the collision coupling model, the fit performs well except for one case, $p = 90$. Although the simulated data do seem to follow the shape of the fit, the data doesn't comply with the $A(\mathrm{N_M}) = 0.5$ criteria, thus this fit is not suitable for p-values of 90 and higher.

In figure 16(a), the fitting parameter c of equation 45 is plotted against p, again with error bars with the size of one standard deviation.

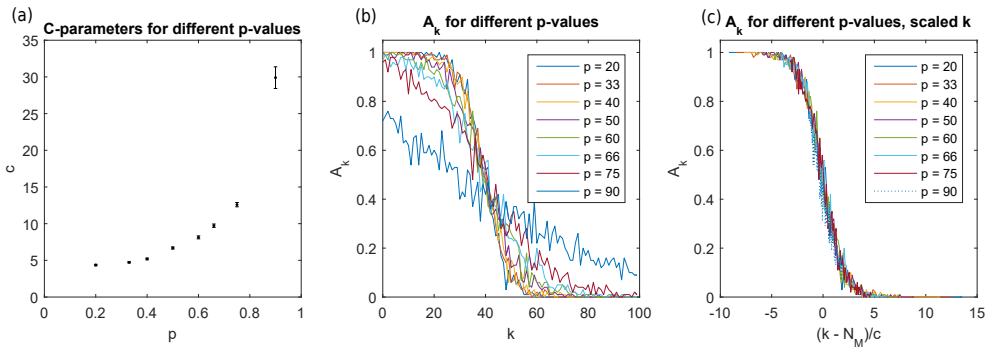

Figure 16: Scaling in the precoupling model, in (a) the best fit-parameter to equation 45 is shown for different p-values. In (b) the simulation results are shown for different p-values and (c) shows the same results, after scaling the k-axis with the c corresponding to the used p-value.

In this plot it's visible that only for $p = 75, 90$, c is too big to make the error in I in equation 46 over 2%. We have $\frac{N_M}{c} = 3.2$ and 1.3 respectively, which makes the errors in I 2.2% and 8.8%

In figure 16(b) all graphs of figure 15 are shown in one figure, after offsetting and scaling the k parameter, the plots overlap fairly well, this can be seen in figure 16(c). Note that although the fit for $p = 90$ was not great, the found scaling parameter still makes A_k behave similar to the others.

For the same reason that c was decreasing when p is increasing in the collision coupling model, we see that c decreases when p increases here. We again give a best guess for the relation between c and p:

$$c(p) = \exp(ap^2) + b, \text{ with } a = 4.04 \pm 0.03 \text{ and } b = 3.5 \pm 0.2 \tag{47}$$

4.4. Influences across the membrane

For the next section, the analyses are done based on the equations from section 2.4 and 2.5. We will take $p = 0.5$ as the standard value.

Collision Coupling

In figure 17(a) we see a comparison between the results of the model as described in section 2.4, the impact of receptors with the same statistics on each other, and the model from 2.3, the independent simulated patches. The results overlap as expected, just 6% of the data points are more than 2 standard deviations apart from each other (with only 1% over 3 standard deviations apart), which means that the assumption that patches could be modeled independently is confirmed.

In figure 17(b) we see a comparison between the signal of the receptor R_{in} with the higher p-value and the signal of a receptor in its environment (a receptor from R_{out}, located as far as possible from R_{in}). Normally A_k drops more quickly as the p-value of the receptor rises (see figure 12(b)), when the patches with different p-values are connected this isn't true anymore. In figure 17(b), A_k for the receptor R_{in} is higher for almost all k. This is a consequence of the 'stolen particle - principle' as described in section 3.2. The main reason that A_k drops more quickly with a higher p in the isolated patches model, is because too many messenger molecules are used for detecting the first few ligand molecules. Upon connecting the patch to an environment where less messenger molecules per time unit are absorbed, it will steal those molecules, resulting in a higher detecting probability.

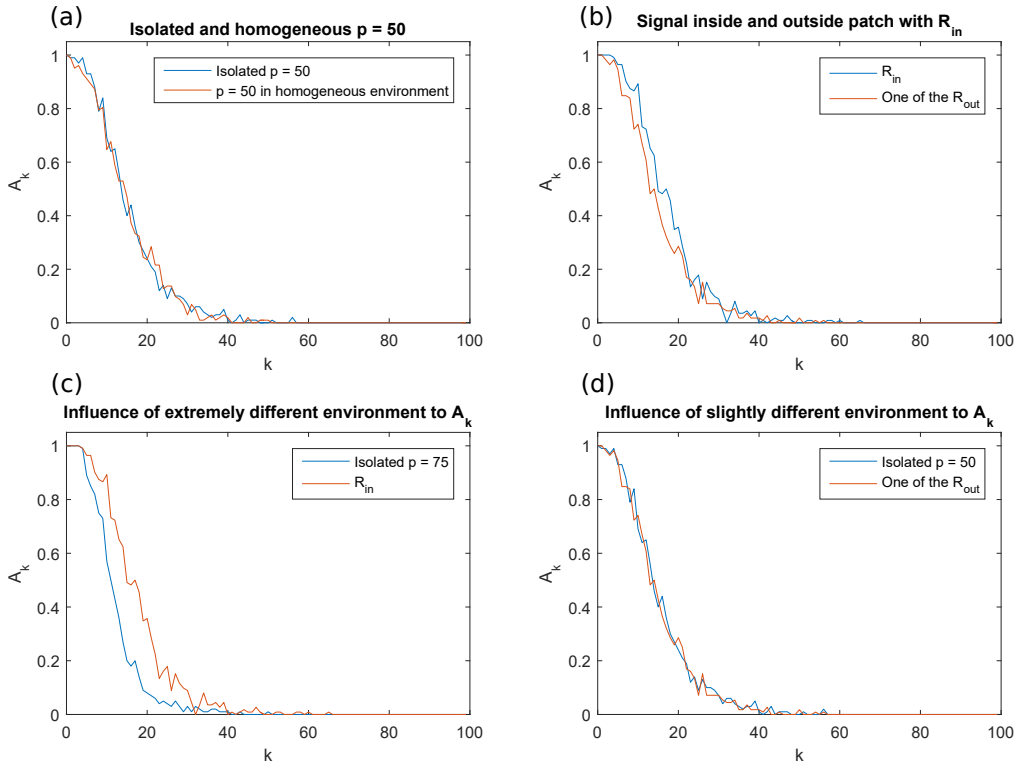

Figure 17: Simulations on the influence of the environment outside a patch to the signal inside it using the collision coupling model, in (a) a isolated patch is compared to a patch who has neighbours with exactly the same receptor statistics. In (b) R_{in} and one of the receptors from its environment R_{out} are compared. In (c) we compare a isolated $p = 75$ receptor to a $p = 75$ receptor in an environment of only $p = 50$ receptors. In (d) we compare a isolated $p = 50$ receptor to a receptor with $p = 50$ in an environment of 23 other $p = 50$ receptors and one $p = 75$ receptor.

The differential equation from section 3.2 predicts that the total amount of messenger molecules absorbed in R_{in} would be $n = 58.8 = 1.47\text{N}_{\text{M}}$, the simulation results were that $n = 56.7 = 1.41\text{N}_{\text{M}}$.

In figure 17(c) we see that a big difference is visible between two receptors (with $p = 75$) in different environments. Due to a stream of extra messenger molecules, the receptor which is surrounded by receptors with lower p-values is able to detect more accurately for a longer period of time. However the reverse influence (figure 17)(d)) of the one higher p-value to its environment is not noticeable at all. The reason for this is that the messenger molecules which are being stolen are from all surrounding patches, in figure 8(b) the effective amount of messenger molecules per receptor R_{out} is $n = 39.2 = 0.98\text{N}_{\text{M}}$. Resulting that per patch almost no difference in A_k can be seen. The diffusion rate is high enough that analyzing a patch closer to the the patch with R_{in} will make little difference.

Precoupling

For a fair analysis between the two models, we again want the probability of an absorption in receptor R_{in} 1.5 times as high as the probability of an absorption in all other receptors (given that the receptor site is not occupied). To accomplish this, we set the p-value of receptor R_{in} to $p = 33$.

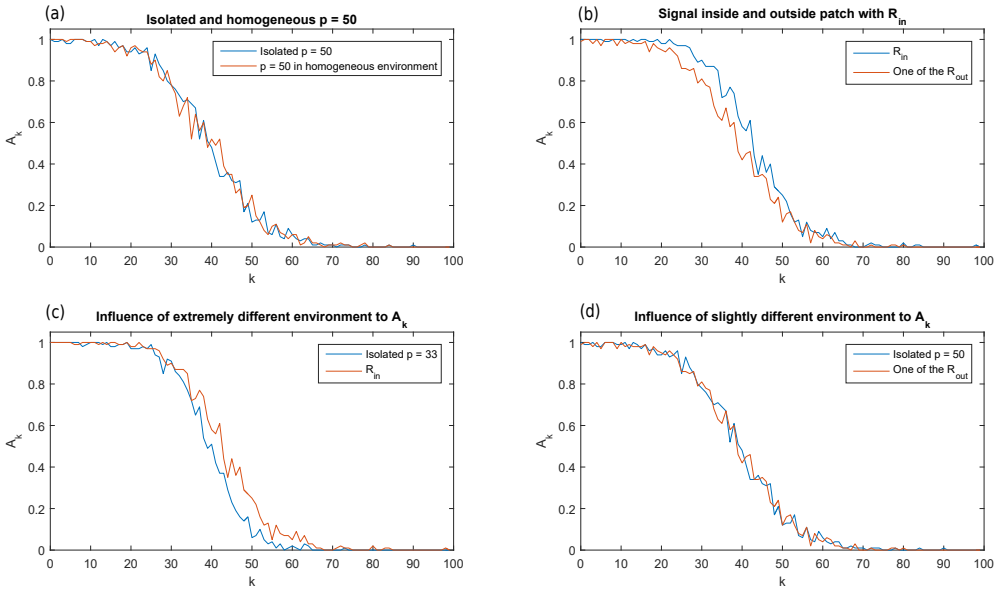

Figure 18: Simulations on the influence of the environment outside a patch to the signal inside it using the precoupling model, in (a) a isolated patch is compared to a patch who has neighbours with exactly the same receptor statistics. In (b) R_{in} and one of the receptors from its environment R_{out} are compared. In (c) we compare a isolated $p = 33$ receptor to a $p = 33$ receptor in an environment of only $p = 50$ receptors. In (d) we compare a isolated $p = 50$ receptor to a receptor with $p = 50$ in an environment of 23 other $p = 50$ receptors and one $p = 33$ receptor.

In figure 18 we have 4 plots similar to the plots in figure 17. Plot (a) again confirming that the patches can be simulated independently in homogeneous environments. And figure 18(d) shows that also for the precoupling case the influence of one different receptor is not measurable in its environment.

Figure 18 shows that A_k will be higher for the receptor R_{in} for all k, which is not what we saw when the patches were simulated individually. In figure 16 the trend is, that for lower p, A_k is higher for $k < 40$ and lower for $k > 40$, upon connecting patches with different receptor statistics, this crossover at $k = 40$ disappears.

In figure 18(c), we find again that the environment of a receptor has a big influence on the receptor signal (A_k) it produces, if a receptor is connected to other receptors with in this case higher p-values, it will detect more accurately for a longer period of time than when it's connected to other receptors with the same p-value.

The reason for this is again, if the receptor is connected to other receptors with higher p-values, they will exchange messenger molecules. This will lead to a net-gain in total absorbed messenger molecules for the receptor with the lower p-value. In figure 8(b) in section 3.2, it can be seen that the effect of the stealing of particles is smaller for the precoupling model, it will only result in a net gain of about 5% of N_{M}. This smaller effect can be explained by less possibilities for stealing. In the collision coupling model, R_{in} can always absorb messenger molecules. In the precoupling model absorbing a messenger molecule is just possible when R_{in} is not occupied. Typically at the start all receptors are occupied, so absorbing and thus stealing is not possible. This also explains why the stealing doesn't start immediately for the precoupling model (in figure 8(a) n_{in} starts to rise immediately, while in figure 8(b) it starts to rise at $k \approx 20$).

For both models we found that the signal obtained from the receptors is both dependent on the p-value of the receptor and the p-values of the receptors in its environment. This means that the independent patches used in our model are valid just for analyzing under homogeneous circumstances, that is circumstances in which all receptors have similar p and T.

In the collision coupling model we find that more messenger molecules are stolen, which was also seen analytically (figure 8). As a result, the receptor signal shows a bigger difference when surrounded by receptors with different p-values, compared to a receptor surrounded with receptors with identical p in the collision coupling model (we see a bigger difference in figure 17(c), than in figure 18(c)). However, across the membrane the difference seem to be of similar size (figure 17(b) and 18(b)).

4.5. Returning Messenger Molecules

As the amount of time it takes for messenger molecules to get back to the membrane is unclear, a few different orders of T_r will be analyzed. In this section we will again use $p = 0.5$ for all simulations.

Region (1): $T_r \leq 1$

This region of T_r is straightforward. As the messenger molecules come back so quickly that there will always be just below N_M messenger molecules on the membrane. As the amount of messenger molecules on the membrane is the only variable that makes A_k go down with time, this means that A_k will be constant from the start.

Evaluating equation 37 and solving equation 36 when it's equated to 40 for $T_r = 1$, tells us that an equilibrium is reached with $n_e = 39.0$ in the precoupling model and $n_e = 34.4$ in the collision coupling model. The expected long term limits for A_k in the precoupling and collision coupling model are both 0.997. This equilibrium is reached almost immediately.

Region (2): $1 < T_r \leq 10$

After evaluation of the same equations as in region 1, we expect region 2 to be more interesting. For $T_r = 6$, the analytic expressions tell us that an equilibrium is expected with $n_e = 34.0$ and $n_e = 20.3$, for the precoupling and collision coupling model respectively. With A_k nearing 0.993 and 0.94 at equilibrium.

This equilibrium is still reached quickly. The numeric results for the precoupling model agree with the analytic results. We find $A_k = 0.995$. However for the collision coupling model we find $A_k = 0.965$. The figures corresponding to this region can be found in the appendix D.

The standard deviations in the simulated values for A_k are 0.001 for the precoupling model and 0.002 for the collision coupling model. Which tell us that the simulated results in the collision coupling model are too far from what we analytically expected.

Region (3): $10 < T_r \leq 100$

The most interesting region, is the region in which the replacement time is from the order 10, here the replacement time is such that equilibrium isn't found immediately, which means that for small k the features we found in section 4.3 can be seen, and for large k an equilibrium will be found.

We take $T_r = 60$ and we follow the same procedure of first analyzing the analytic expressions. For the precoupling model we find the equilibrium at $n_e = 5.3$ and $A_k = 0.511$, while for the collision coupling model we find $n_e = 3.8$ and $A_k = 0.476$. The numeric results give that for the precoupling model $A_k = 0.569$ and for the collision coupling model this equilibrium is found at $A_k = 0.463$.

With an standard deviation of 0.007 for both the precoupling model and the collision coupling model. In this region the difference between the analytic result and the simulations is over 2 standard deviations for the precoupling method.

In figure 19(a) and 19(b) you can see that the initial response for both models is the same as the models without the replacing of the messengers. However a little after $k = 60$, the first messenger molecules are being replaced on the membrane, creating a new peak. Which is less high and broader than the first peak. This process will repeat at $k = 120, 180, \ldots$ with each peak getting less high and broader, until the system reaches its equilibrium. Which is depicted in figure 19(c) and figure 19(d).

Region (4): $T_r \geq 100$

In this region, you will just get the same figures as in figure 11 and 15 for the initial response. The time it will take for messenger molecules to get replaced is so long that in our analysis, which contains the first 100 bound ligands, it will not be seen.

We make an estimate for the equilibrium values in this region. We take $T_r = 600$ and analyze the analytic expressions of section 3.3 again. We find that for the precoupling model we expect an equilibrium with $n_e = 0.42$ and $A_{k_e} = 0.064$. For collision coupling we find $n_e = 0.41$ and $A_{k_e} = 0.062$. Which means that at equilibrium for used parameters only 6% of the ligand will get detected in both models.

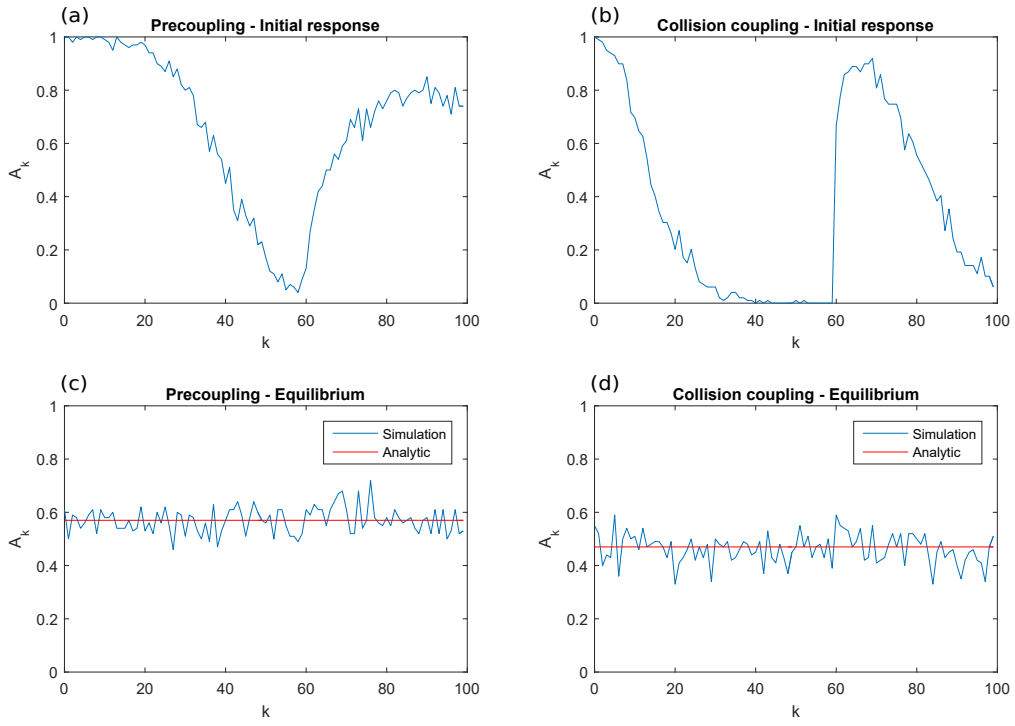

Figure 19: Influence of replacing messenger molecules with a replacing time of 60 k-phases. In (a) the initial response is visible for the precoupling model, which means that the patch has all messenger molecules in its system when suddenly its receptor starts binding ligand with $p = 50$, in (c) we see what happens at equilibrium. (b) and (d) show the same responses as (a) and (c) respectively, but for the collision coupling model. In (c) and (d) the results to the analytic equations discussed in section 3.3 are added as well.

In the 4 regions, we saw that when the replacement time is too low, the features discussed in earlier sections are lost. Independent of the p-value, A_k will stay close to 1, making it harder to determine the outside ligand concentration. Further, we saw that the equilibrium is both higher and reached earlier in the precoupling model. This means that for higher replace times, A_k will still always be close to 1 in the precoupling model, while different p-values can already be distinguished from each other for the collision coupling model (see region 2).

DISCUSSION

5.1. CONCLUSION

In this research, we built upon the model from Hille and Dubbeldam [1], after concluding that a simpler way of modelling the receptor state did not influence the receptor signals for the independent patches, we extended the model to research both the influence of surrounding receptors and the influence of returning messenger molecules to the membrane.

For the influence of surrounding patches, we conclude that the statistics of receptors in patches in the environment of a given receptor are as big of a influence to the receptor signal as the statistics of the receptor itself. The two main variables that determine the receptor signal at a given time, are the p-value of the receptor and the amount of messenger molecules close to the receptor. The latter of the two is determined by a combination of the receptor itself and the receptors in neighbouring patches, giving those neighbouring receptors a crucial role in determining the receptor signal of the given receptor. In the collision coupling model, the influence of the neighbouring receptors to the receptor signal was slightly larger. Therefore, this model is more accurate at detecting differences in p-values of different receptors.

The exact influence of returning messenger molecules remained unclear, since the replace rate with which the messenger molecules returned is unknown. However because this rate is thought to be a few orders larger than the typical bind and unbind time of a ligand molecule, we expect that the returning of the messenger molecules will at first cause the receptor signal to fluctuate heavily, creating multiple peaks with the height (in detecting probability) decreasing and width (in time) increasing until it finally reaches an equilibrium. This equilibrium will in general be higher and reached more quickly for the precoupling model, which means that at low replace rates it will become harder for the precoupling model to determine where the ligand concentration is the highest.

5.2. SCALING

The scaling parameters we found in section 4.3 perform as desired and they seem to follow a certain pattern in both models. Still the questions remain: What pattern do the scaling parameters follow exactly and why do they follow these patterns? In section 4.3 we give a guess of the relation between p and c, but we do not explain why this pattern is followed. Only an explanation on the decreasing form of the relation between p-value and scaling parameter in the collision coupling model and the increasing form of this relation in the precoupling model is made.

5.3. AMBIGUITY IN PRECOUPLING METHOD

In section 4.4 we find that in the precoupling model that the receptor signal can be interpreted in multiple ways, depending on conditions of ligand molecules outside of the membrane. To see this, we will sketch two scenarios.

If we assume concentrations as in this report, so that receptors are occupied on average for half the time. To find where on the membrane receptors are typically bound the most, we would pick the part of the membrane with the lowest receptor signal, which was also found in the precoupling part of section 4.4. In contrary, if we assume extreme low concentrations, so that only very occasionally receptors are bound. Then the only receptor signal generated will be by those occasional bindings. In this case the receptors generating the most signal will have the highest receptor occupation.

Because of this, the precoupling method is expected to only operate in low concentrations, detecting the receptors which are unbound a large fraction of time. This is especially important when combining the precoupling and collision coupling mechanisms so that they cooperate, the receptors which are able to precouple messenger molecules are then responsible for detecting the low ligand concentrations.

5.4. FURTHER RESEARCH

An possible extension to the model from section 2.5 is the movement of receptors. We know that the messenger molecules are not the only moving particles on the membrane, the receptors are also moving, although this movement is slower. A reaction with a messenger molecule slows the receptor down. This would result in receptors moving with high speed in zones where little ligand is available, and low speed in zones where the ligand molecules are more concentrated. Resulting in higher concentrations of receptors at the part of the membrane with higher ligand concentration. With this model, the part of the membrane with the highest receptor concentration would give us the direction in which the cell should move.

Throughout this entire report, when discussing the collision coupling model, we neglected the amount of messenger molecules activated per ligand bound, since the measure we analyzed did not take this in account. It is clear that no extinction can be made between the messenger molecule that first detected a ligand or other messengers who detected it later. Which might mean that an analysis on this topic would give us some insight in the chemotaxis of *Dictyostelium discoideum*.

Another obvious research topic this paper would benefit from is an estimate to the replace rate of the messenger molecules, that is the time it will take G_α to get back to the membrane, meet with a $G_{\beta\gamma}$ and combine to a $G_{\alpha\beta\gamma}$. In section 4.5 we saw that if the replace rate is small ($T_r \leq 10$) an equilibrium is reached quickly and the details seen in 4.3 are not relevant anymore.

A last possible extension is a model in which the precoupling model and the collision coupling model are combined. As discussed in the ambiguity of the precoupling method (section 5.3), cells have a combination of precoupling and collision coupling receptors. In this extension, the precoupled receptors will detect accurately in low concentrations of ligand, while the collision coupled receptors will detect accurately in high concentrations.

BIBLIOGRAPHY

[1] Hille, S.C. and Dubbeldam, J.L.A (201x). A quantitative comparison of signal transduction fidelity between two chemo-reception mechanisms. *Unpub.*.

[2] Kollmann, M., Løvdok, L., Bartholomé, K., Timmer, J. and Sourjik, V (2005). Design principles of a bacterial signalling network, *Nature* vol. 438, pp. 504–507.

[3] Kitano, H. (2004). Biological robustness. *Nature Rev. Genet.* vol. 5 pp. 826–837.

[4] Stock, J.,Levit, M. and Wolanin, M. (2002). Information Processing in Bacterial Chemotaxis, *Sci. STKE* vol. 132, pp. 25.

[5] Aquino, G., Wingreen, N.S. and Endres, G.R. (2016). Know the Single-Receptor Sensing Limit? Think Again, *J Stat Phys* vol. 162, pp. 1353-1364.

[6] Berg, H.C. and Purcell, E.M. (1977). Physics of chemoreception, *Biophys J.* vol. 20, pp. 193-219.

[7] Endres, G.R. and Wingreen, N.S (2008). Accuracy of direct gradient sensing by single cells, *Proc. Natl. Acad. Sci. USA* vol. 105, pp. 15749–15754.

[8] Endres, G.R. and Wingreen, N.S. (2009). Maximum likelihood and the single receptor, *Phys. Rev. Lett.* vol. 103, pp. 158101.

[9] Hille, B. (1992). G protein-coupled mechanism and nervous signalling, *Neuron* vol. 9 pp. 197-195.

[10] Nobles, M., Benians, A., and Tinker, A. (2005). Heterotrimeric G proteins precouple with G protein-coupled receptors in living cells, *PNAS* vol. 102, pp. 18706-18711.

[11] Fisher, P.R., Merkel, R. and Gerisch, G. (1989). Quantative analysis of cell motility and chemotaxis in Dictyostellium discoideum by using an image processing system and a novel chemotaxis chamber providing stationary chemical gradients, *J. Cell Biol.* vol. 108 pp. 973-984.

[12] Song, L., Nadkarni, S.M., Bödecker, H.U., Beta, C., Bae, A., Franck, C., Rappel, W.J., Loomis, W.F. and Bodenschatz E. (2006). Dictyostelium discoideum chemotaxis: threshold for directed motion, *Eur. J. Cell Biol.* vol. 85, pp. 981-989.

[13] Arkowitz, R.A. (1999), Responding to attraction: chemotaxis and chemotropism in Dictyostelium and yeast, *Trends in Cell Biology* vol. 9 pp. 20-27.

[14] Mato, J.M., Losada, A., Nanjundiah, V. and Konijn, T.M. (1975), Signal input for a chemotactic response in the cellular slime mold Dictyostelium discoideum, *PNAS* vol. 72 pp. 4991-4993.

[15] Stock, A.M., Robinoson, V.L. and Goudreau P.N. (2000), Two-component signal transduction, *Ann Rev. Biochem.* vol. 69 pp. 183-215.

[16] Løvdok, L., Kollmann, M. and Sourjik V. (2007), Coexpression of signaling proteins improves robustness of the bacterial chemotaxis pathway, *J. Biotechn.* vol. 129 pp. 173-180.

[17] Shinar, G., Milo, R., Martínez, M.R. and Alon, U. (2007), Input-output robustness in simple bacterial signaling systems, *Proc. Nat. Acad. Sci. USA* vol. 104 pp. 19931-19935.

[18] Keijzer, S. de et al. (2008), A spatially restricted increase in receptor mobility is involved in directional sensing during Dictyostelium discoideum chemotaxis, *J. Cell Sci.* vol. 121, pp. 1750-1757.

[19] Santillán, M. (2008), On the Use of the Hill Functions in Mathematical Models of Gene Regulatory Networks *Math. Model. Nat. Phenom.* vol. 3, pp. 85-97.

A

Proof regarding the analytic expressions for the collision coupling model

We will proof that equation:

$$P(T_i \in I_k) = b\left(1 - \sum_{j=1}^{k-1} P(T_i \in I_j)\right) \tag{A.1}$$

Is equal to equation:

$$P(T \in I_k) = b(1-b)^{k-1} \tag{A.2}$$

By realizing that according to the binomial theorem we find that equation A.2 can be rewritten as:

$$P(T_i \in I_k) = b\sum_{j=0}^{k-1}\left(\binom{k-1}{j}(-b)^j\right) \tag{A.3}$$

We will continue by proving that A.1 and A.3 are equal by induction. In this section we will shorten $P(T \in I_k)$ by P_k.

Base case: For $k = 1$, we have for A.1: $P_1 = b$ and for A.3 $P_1 = b$, so for $k = 1$, the two equations yield the same result: The base case is confirmed.

Induction hypothesis: Assume that for all $j <= k$ equation A.3 holds.

Induction step: We now need to proof that equation A.3 also holds for $k+1$. We will evaluate P_{k+1} by equation A.1 which gives us:

$$P_{k+1} = P_1\left(1 - \sum_{j=1}^{k} P_k\right)$$

By applying our induction hypothesis:

$$P_{k+1} = b\left(1 - \sum_{j=1}^{k} b\sum_{i=0}^{j-1}\left(\binom{j-1}{i}(-b)^i\right)\right)$$

By taking the minus-sign in front of the first sum and the b-term in front of the second sum into both the sums, and by substituting $m = i+1$ we find:

$$P_{k+1} = b\left(1 + \sum_{j=1}^{k}\sum_{m=1}^{j}\left(\binom{j-1}{m-1}(-b)^m\right)\right)$$

Now we will evaluate the coefficient of each power of b in the double sum individually. By selecting an arbitrary $m_0 \in \{1, ..., k-1\}$. In the second sum, this term will only occur when $j => m_0$, and for those values it will only occur if $m = m_0$, so if we denote the coefficient of $(-b)^{m_0}$ by c_{m_0} we get:

$$c_{m_0} = \sum_{j=m_0}^{k} \binom{j-1}{m_0-1}$$

We know from the Hockey-stick identity that:

$$c_{m_0} = \sum_{j=m_0}^{k} \binom{j-1}{m_0-1} = \binom{k}{m_0}$$

Applying these results to our expression for P_{k+1} gives us:

$$P_{k+1} = b\left(1 + \sum_{j=1}^{k} \binom{k}{j}(-b)^j\right)$$

The final step is realizing that $1 = \binom{k}{0}(-b)^0$ and thus can be brought under the sum for $j = 0$ to get:

$$P_{k+1} = b\sum_{j=0}^{k} \binom{k}{j}(-b)^j$$

So equation A.3 also holds for $k+1$ and by induction it is valid for every value of k, now we have seen that equation A.3 is just the binomial expansion of equation A.2. We conclude that A.1 and A.2 are indeed equal.

B

Figures of receptor signal with Poisson generated on and off times

Simulation results collision coupling

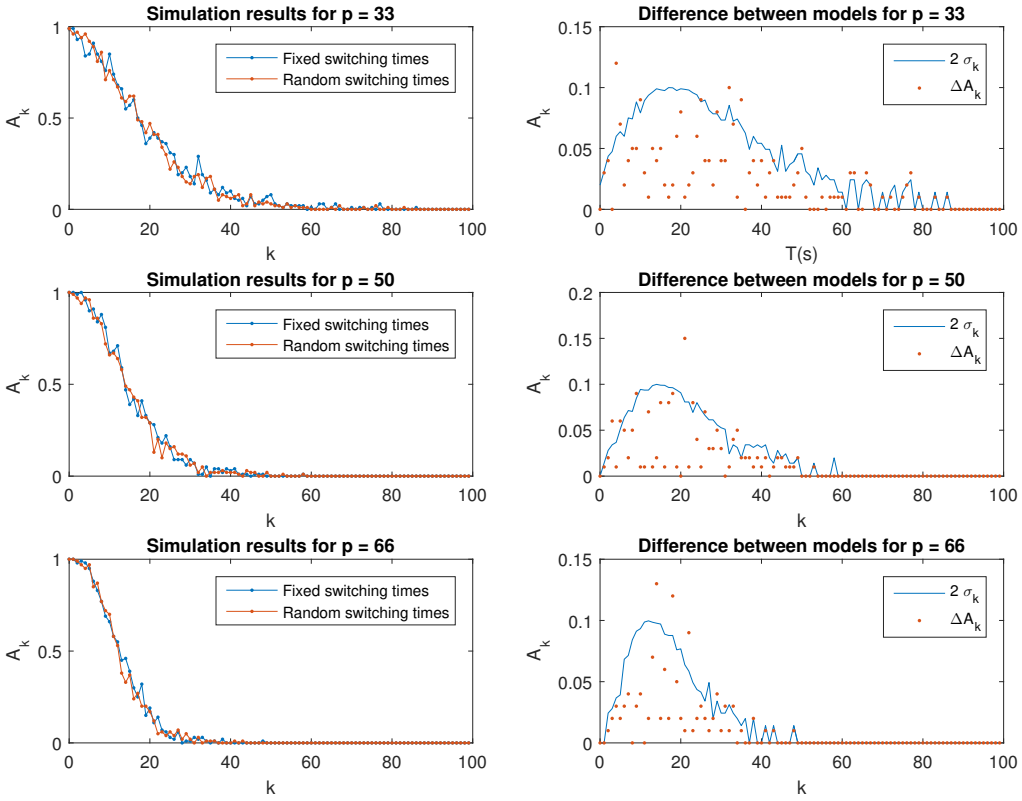

Figure B.1: Comparison between the model using fixed switching times and the model using Poisson distribution generated switching times as parameter for the collision coupling model. The corresponding values for T_{on} and T_{off} can be calculated by $T_{\text{on}} = pT$ and $T_{\text{off}} = (1-p)T$. On the left the results for both models are displayed, on the right the differences between the model and the standard deviation of the data are shown.

Simulation results precoupling

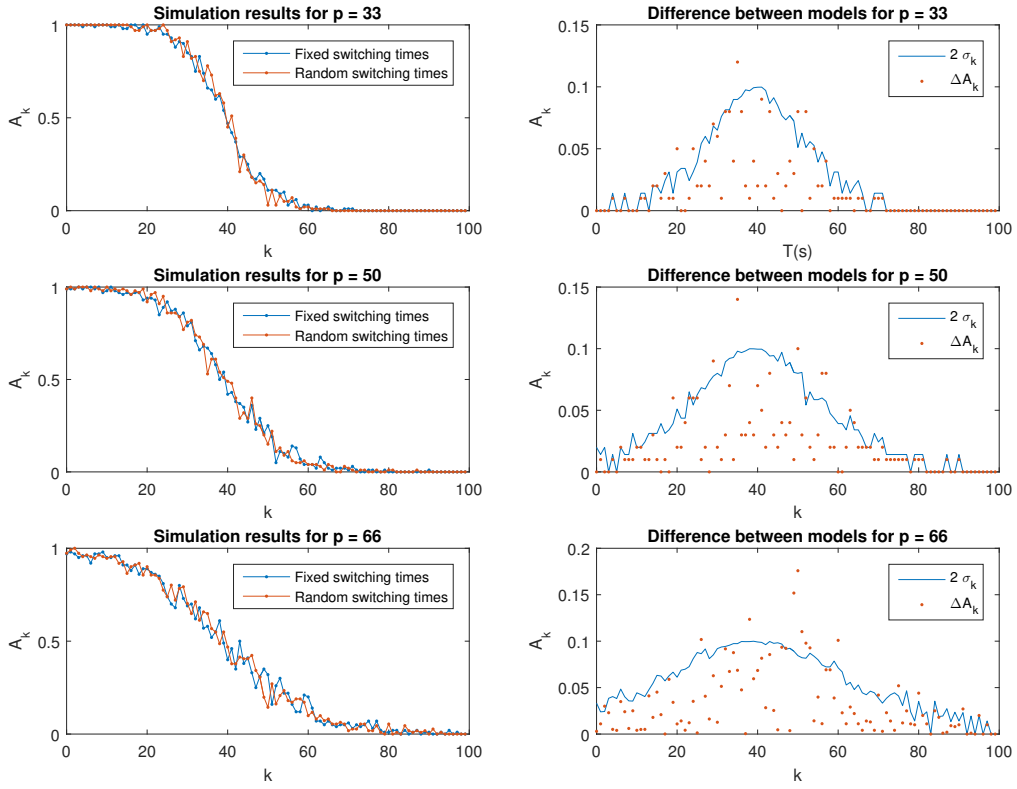

Figure B.2: Comparison between the model using fixed switching times and the model using Poisson distribution generated random switching times as parameter for the precoupling model. The corresponding values for T_{on} and T_{off} can be calculated by $T_{\text{on}} = pT$ and $T_{\text{off}} = (1-p)T$. On the left the results for both models are displayed, on the right the differences between the model and the standard deviation of the data are shown.

C

Comparison of equations collision coupling model

$$A_k = 1 - \left(1 - b(1-b)^{k-1}\right)^{N_M} \tag{C.1}$$

$$A(k) = \exp\left(-\left(\frac{x}{c}\right)^2\right) \tag{C.2}$$

Since an analytic comparison is not possible due to the complexity of equation C.1, we will compare the two for 3 values of p. For this we use the same constants as in section 4. We will compare the equations by normalizing both of them, treat them as probability distributions and then compare their first 3 moments.

Table C.1: Moment comparison of the analytic expression for A_k for the collision coupling model, and the equation used for the scaling of the data

p	b	c	M_1^a	M_1^f	M_2^a	M_2^f	M_3^a	M_3^f
0.33	0.101	21.3	13.1	12.0	294	226	9100	5420
0.50	0.149	18.1	9.47	10.2	147	164	3100	3360
0.67	0.194	14.9	7.52	8.38	90.9	110	1463	1850

In table C.1 the M_i^s denotes the i-th moment of the analytic equation (C.1) when $s = a$, and the i-th moment of the fit-equation (C.2) when $s = f$. In this table we would like $M_i^s = M_i^f$ for all i, for them to be equal. However, we see that this does not hold up, in fact the errors in the 3rd-moments of the fitted curve can get as large as 40% of the analytic moments. We conclude that the expressions show some similarity in form, but details are not preserved. This was also seen in the graphic visualizations from figure 11 and 13. The similarity showed to be enough for the purposes in this research.

D

HIGH REPLACE RATES

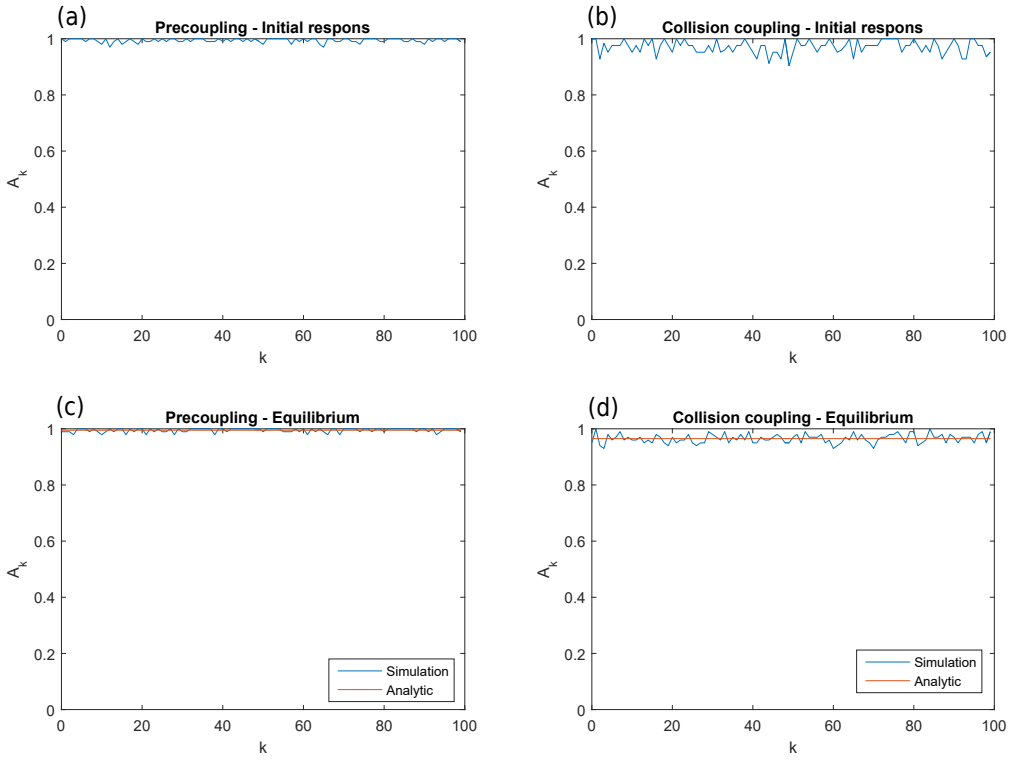

Figure D.1: Influence of replacing messenger molecules with a replacing time of 6 k-phases. In (a) the initial response is visible for the precoupling model, which means that the patch has all messenger molecules in its system when suddenly its receptor starts binding ligand with $p = 50$, in (c) we see what happens at equilibrium. (b) and (d) show the same responses as (a) and (c) respectively, but for the collision coupling model. In (b) and (d) the results to the analytic equations discussed in section 3.3 are added as well.

In figure D.1 almost no difference is visible between the initial response and the response at equilibrium. The replace rate is high enough that messenger molecules come back before the receptor detecting probability drops significantly. This means that in this region, the p dependent dropping receptor responses we have seen so far will not occur in neither the precoupling nor the collision coupling model.